Dual Quaternions as a Tool for Modeling, Control, and Estimation for Spacecraft Robotic Servicing Missions

Article *in* Journal of the Astronautical Sciences · July 2019

DOI: 10.1007/s40295-019-00181-4

Panagiotis Tsiotras
Georgia Institute of Technology

Alfredo Valverde
Georgia Institute of Technology

Dual Quaternions as a Tool for Modeling, Control, and Estimation for Spacecraft Robotic Servicing Missions

Panagiotis Tsiotras* **and Alfredo Valverde**†

ABSTRACT

In recent years there has been an increasing interest in spacecraft robotic operations in orbit. In fact, several agencies and organizations around the world are investigating satellite proximity operations as an enabling technology for future space missions such as on-orbit satellite inspection, health monitoring, surveillance, servicing, refueling, and optical interferometry, to name a few. Contrary to more traditional satellite applications, robotic servicing requires addressing both the translational and the rotational motion of the satellite at the same time. One of the biggest challenges for these applications is the need to simultaneously and accurately estimate – and track – both relative position and attitude reference trajectories in order to avoid collisions between the satellites and achieve stringent mission objectives.

Motivated by our desire to control spacecraft motion during proximity operations for robotic in-orbit servicing missions which do not depend on the artificial separation of translational and rotational motion, we have recently developed a complete theory to describe the 6-DOF motion of the spacecraft using dual quaternions. Dual quaternions emerge as a powerful tool to model the pose (that is, both attitude and position) of the spacecraft during all phases of the mission under a unified framework. In this paper, we revisit the basic theory behind dual quaternions and the associated Clifford algebras and we use this mathematical tool to derive several spacecraft pose controllers as well as pose estimation filters. We show that the resulting mathematical structure lends itself to the straightforward incorporation of an adaptive estimation scheme known as concurrent learning, which allows us to also estimate on-the-fly the mass properties of the spacecraft.

Key words: Dual quaternions - Concurrent learning - Estimation - Robotic servicing

INTRODUCTION

Satellite in-orbit servicing has a rather long history dating back at least to the 1970's. Many – but not all – in-orbit servicing missions include a satellite with a robotic manipulator. Other in-orbit servicing missions include operations

*David and Andrew Lewis Chair Professor, School of Aerospace Engineering, and Institute for Robotics and Intelligent Machines, Georgia Institute of Technology.

†Ph.D. Student, School of Aerospace Engineering, Georgia Institute of Technology

between two or more satellites flying in close proximity. In either case, satellite servicing includes active control both of the relative orientation as well as the relative position of the satellite.

The first robotic arm used on a robotic (or unmanned) satellite was the Engineering Test Satellite No. 7 (ETS-VII) launched in 1997 by the National Space Development Agency of Japan (NASDA). Among the many tests performed, the arm was successfully used for the capture of a target satellite with a teleoperated chaser.[1,2] In 2007, DARPA's Orbital Express Demonstration System was launched with the objective of performing in-orbit satellite refueling, among a host of other autonomous operations using a 6-DOF manipulator.[3,4]

Current efforts go beyond mere conceptual testing, into the realm of standardization and profitability. Henshaw describes the Front-end Robotics Enabling Near-term Demonstration (FREND) program for the demonstration of autonomous rendezvous and docking for the capture and orbit elevation of GEO satellites.[5] The FREND program was sponsored by DARPA, and developed by the Naval Research Laboratory (NRL). Roesler[6] describes the follow-up Robotic Servicing of Geosynchronous Satellites (RSGS) program, also developed by DARPA as an effort "[t]o create a dexterous robotic operational capability in Geosynchronous Orbit, that can both provide increased resilience for the current U.S. space infrastructure, and be the first concrete step toward a transformed space architecture with revolutionary capabilities." This statement closely aligns with the National Space Policies published in 2010.[7] With the RSGS program, DARPA aims at establishing a government-led cohort of companies to develop their own servicing satellite for GEO. After the accomplishment of mission-independent milestones set by DARPA, the participating companies will be sent off to profit by servicing existing satellites. In a similar effort, the Restore-L mission by NASA aims at developing a suite of tools for on-orbit refueling of a government-owned satellite in polar orbit.[7,8]

Satellite robotic arms are not limited to capturing space assets or just performing minor servicing operations. Their availability in space opens a gamut of possibilities that include in-space assembly of large structures, payload transfer between orbiting satellites, rescue missions of stranded space vehicles, effective momentum transfer of a detumbling spacecraft, debris capture, just to name a few.[9–11] Other possible uses include robot-wielding satellites capturing an asteroid that threatens colliding with the Earth and then redirecting it towards a safe orbit.

In-orbit robotic servicing poses many challenging questions in terms of modeling, control, and estimation. The primary one – already alluded to – is the fact that the dynamics of the robotic arm and the satellite base are tightly coupled and hence in order to achieve precise end-effector control, robotic servicing missions require accounting for the satellite's position, not only its attitude. Although decoupling the translational and the rotational motion is sometimes justified, a more holistic approach that captures the combined motion is more realistic and will potentially lead to better performance. Several approaches have been used to model the combined, coupled motion of a satellite-mounted robotic manipulators in-orbit, but control design for the combined motion still remains challenging. In this work, in order to simplify the controller development, and for reasons that will become apparent shortly, we advocate the use of dual quaternions as the parameters of choice to describe the 6-DOF motion of the satellite. Although dual quaternions have been used extensively in the (ground) robotics community,[12] their use for describing the motion of satellites in orbit is fairly recent. This is rather surprising, given the success quaternions have had for solving many real-life attitude control and estimation problems . Dual quaternions, owing to their similarity to regular quaternions, arise naturally as the prime candidate to address many combined spacecraft pose control and estimation problems that are very common in spacecraft servicing missions and similar proximity operations.

Among the several contributions in the dual quaternion literature we mention Brodsky and Shoham,[13] who provided an in-depth introduction to the use of dual number theory for the modeling of dynamical systems, as well as for the treatment of functions of dual variables, and Dooley and McCarthy[12] who used dual quaternions as generalized coordinates in Kane's method to describe the 6-DOF dynamics of a single rigid body. The Newton-Euler view of rigid body rotational dynamics using dual quaternions was first derived in References 14 and 15, providing powerful insights into the analogies that exist between modeling rotational-only or rotational-and-translational dynamics respectively, and even deeper implications in terms of control. Wang and Yu[16] proposed a PID controller based on dual quaternions. Wang et al[15,17] made use of dual quaternion algebra to establish finite-time controllers for relative navigation. Filipe et al[18–21] and Seo[22] proposed a series of control laws that perform pose-tracking, while Lee and Mesbahi[23–25] introduced dual quaternions for modeling convex constraints in an MPC control formulation.

The goal of this paper is two-fold. First, for the uninitiated reader, we provide an overview of quaternions and dual quaternions and show their links with each other and with the underlying mathematical framework they are part of, namely, Clifford Algebras. This is followed by an overview of recent work that exploits the structural similarities between quaternions and dual quaternions for 3-DOF and 6-DOF motion, respectively. The second objective is to introduce a new 6-DOF adaptive pose tracking controller in terms of dual quaternions that makes use of concurrent learning, a relatively new technique to augment adaptive controllers with on-line model learning ideas. We show that concurrent learning aids in the convergence of the estimation of the mass and inertia properties of the system beyond what traditional persistency of excitation can achieve. We conclude with a numerical comparison of the proposed controller with a controller that does not make use of concurrent learning to demonstrate the benefits of the proposed approach.

MATHEMATICAL PRELIMINARIES

Clifford Algebras

A Clifford algebra is generated from a vector space endowed with a geometric product. The geometric product is defined from a quadratic form and, as a result, often one only needs to define the quadratic form and the underlying vector space to construct the associated Clifford algebra. Specifically, the Clifford algebra is a unital and associative algebra over a vector space V with a quadratic form $v^2 = Q(v),\ v \in V$. Every non-degenerate quadratic form over a finite-dimensional real vector space can be expressed in the form

$$Q(v) = v_1^2 + \cdots + v_p^2 - v_{p+1}^2 - \cdots - v_{p+q}^2, \tag{1}$$

where $n = p + q$ is the dimension of the vector space. The quadratic form Q is usually associated to the symmetric bilinear form F, defined via the polarization identity

$$F(u,v) = \frac{1}{2}\left(Q(u+v) - Q(u) - Q(v)\right), \tag{2}$$

so often one is given the bilinear form F instead of the quadratic form Q. The basis elements of a Clifford algebra are constructed from the basis elements of V using the following process. Let $\{\mathbf{e}_1, \ldots, \mathbf{e}_n\} \subset V$ be the standard basis for the n-dimensional vector space V and let $\mathbf{e}_0 = 1$ be the unit, or scalar. In general, each of these basis elements $\mathbf{e}_i$ satisfies

$$\mathbf{e}_i^2 = \begin{cases} +1, & \text{if} \quad i \in \{1, \ldots, p\}, \\ -1, & \text{if} \quad i \in \{p+1, \ldots, p+q\}, \\ \ \ 0, & \text{if} \quad i \in \{p+q+1, \ldots, n\}. \end{cases} \tag{3}$$

The pairwise product of basis vectors satisfies the anti-commutativity property

$$\mathbf{e}_i\mathbf{e}_j = -\mathbf{e}_j\mathbf{e}_i \quad \text{if} \quad i \neq j. \tag{4}$$

Products of the basis vectors of V form the basis elements, or monomials, of the Clifford algebra. For notational simplicity, this product is often succinctly displayed as

$$\mathbf{e}_{abc\ldots d} \triangleq \mathbf{e}_a\mathbf{e}_b\mathbf{e}_c\ldots\mathbf{e}_d, \qquad \{a, b, c, \ldots, d\} \subseteq \{1, \ldots, n\}. \tag{5}$$

Any product of monomials can be simplified using equations (3) and (4) so that each $\mathbf{e}_i$ appears at most once per element of the Clifford Algebra. If, in addition,

$$\mathbf{e}_{k_1k_2\ldots k_p} \triangleq \mathbf{e}_{k_1}\mathbf{e}_{k_2}\ldots\mathbf{e}_{k_p}, \quad k_i \in \{1, \ldots, n\}, \tag{6}$$

satisfies $0 < k_1 < k_2 < \cdots < k_p$, then we say that $\mathbf{e}_{k_1k_2\ldots k_p}$ is grade-p, or $\mathbf{e}_{k_1k_2\ldots k_p} \in \bigwedge^p V$, the $p-$th exterior algebra of V. The previous notation and terminology stems from the fact $\mathbf{e}_i \wedge \mathbf{e}_j = \mathbf{e}_i\mathbf{e}_j$ for $i \neq j$ and $\mathbf{e}_i \wedge \mathbf{e}_j = 0$ for $i = j$. Elements of the Clifford algebra belonging to V are called vectors (or elements of grade-1), elements belonging to $V \wedge V$ are called bi-vectors (or elements of grade-2), elements belonging to $V \wedge V \wedge V$ are called tri-vectors (or elements of grade-3), etc. Note that scalars are grade-0 elements. The general element of a Clifford algebra is therefore a linear combination of scalars, vectors, bi-vectors, tri-vectors, etc. It is appropriately called a multi-vector.

Clifford algebras are commonly denoted by $C\ell_{p,q,r}(V,Q)$, or $C\ell(p,q,r)$ when the vector space and the quadratic form have been previously defined. The triplet (p,q,r) is the signature of the algebra, and satisfies the equation $n = p+q+r$, where n is the dimension of V. The algebra $C\ell(p,q,r)$ is therefore defined as

$$C\ell(p,q,r) = \bigoplus_{i=0}^{n} \bigwedge^i V. \tag{7}$$

The even-graded elements of $C\ell(p,q,r)$ along with the unit $\mathbf{e}_0$ form a sub-algebra denoted by $C\ell^+(p,q,r)$. Specifcally,

$$C\ell^+(p,q,r) = \bigoplus_{\substack{i=0 \\ i \text{ even}}}^{n} \bigwedge^i V \tag{8}$$

is closed under multiplication since the basis vectors cancel out in pairs.

Quaternions

Consider the algebra $C\ell(0,3,0)$ over $\mathbb{R}^3$ with standard basis elements (or basis vectors) $\{\mathbf{e}_1, \mathbf{e}_2, \mathbf{e}_3\}$ satisfying $\mathbf{e}_1^2 = \mathbf{e}_2^2 = \mathbf{e}_3^2 = -1$ stemming from the quadratic form $Q(v) = -v_1^2 - v_2^2 - v_3^2$ for a given element $v = v_1\mathbf{e}_1 + v_2\mathbf{e}_2 + v_3\mathbf{e}_3 \in V$. The canonical basis for this algebra is given by $\{1, \mathbf{e}_1, \mathbf{e}_2, \mathbf{e}_3, \mathbf{e}_{23}, \mathbf{e}_{31}, \mathbf{e}_{12}, \mathbf{e}_{321}\}$. The highest grade element $\mathbf{e}_{321}$ is called a *pseudoscalar* and is often denoted by $\mathbf{I}$. That is, $\mathbf{I} = \mathbf{e}_{321}$.

From the definition of the basis (5), along with (4), it can be easily shown that

$$\mathbf{e}_{12}^2 = (\mathbf{e}_1\mathbf{e}_2)(\mathbf{e}_1\mathbf{e}_2) = \mathbf{e}_1\mathbf{e}_2\mathbf{e}_1\mathbf{e}_2 = -\mathbf{e}_1\mathbf{e}_1\mathbf{e}_2\mathbf{e}_2 = -\mathbf{e}_1^2\mathbf{e}_2^2 = -(-1)(-1) = -1, \tag{9}$$

and, similarly, $\mathbf{e}_{23}^2 = \mathbf{e}_{31}^2 = -1$. Additionally, it can be shown that the following cyclic relationships hold

$$\mathbf{e}_{23}\mathbf{e}_{31} = \mathbf{e}_{12}, \qquad \mathbf{e}_{31}\mathbf{e}_{12} = \mathbf{e}_{23}, \qquad \mathbf{e}_{12}\mathbf{e}_{23} = \mathbf{e}_{31}. \tag{10}$$

Thus, the geometric product between grade-2 elements yields a scalar (grade-0) as in (9), or another grade-2 blade, as in (10).

The canonical basis for $C\ell^+(0,3,0)$ is therefore $\{1, \mathbf{e}_{23}, \mathbf{e}_{31}, \mathbf{e}_{12}\}$. Any element q in $C\ell^+(0,3,0)$ can therefore be represented as

$$q = q_0 + q_1\mathbf{e}_{23} + q_2\mathbf{e}_{31} + q_3\mathbf{e}_{12}, \tag{11}$$

that is, it is a sum of a scalar (q_0) and a bi-vector ($q_1\mathbf{e}_{23} + q_2\mathbf{e}_{31} + q_3\mathbf{e}_{12}$).

The group of quaternions, as defined by Hamilton in 1866[26] , extends the well-known imaginary unit j, which satisfies $j^2 = -1$. This non-abelian group is defined by $\mathbb{Q}_8 \triangleq \{-1, i, j, k : i^2 = j^2 = k^2 = ijk = -1\}$. The algebra constructed from $\mathbb{Q}_8$ over the field of real numbers is the quaternion algebra defined as $\mathbb{H} \triangleq \{q = q_0 + q_1 i + q_2 j + q_3 k : i^2 = j^2 = k^2 = ijk = -1,\ q_0, q_1, q_2, q_3 \in \mathbb{R}\}$. This defines an associative, non-commutative, division algebra. A quaternion is given by

$$q = q_0 + q_1 i + q_2 j + q_3 k. \tag{12}$$

By comparing (11) and (12) and from the definitions and relationships between the different elements of $C\ell^+(0,3,0)$ and $\mathbb{H}$, it is clear that $C\ell^+(0,3,0) \cong \mathbb{H}$, where the basis elements can be matched as described in Table 1.

Table 1. Matching of Clifford algebra elements and quaternion algebra elements.

$C\ell^+(0,3,0)$	$\mathbb{H}$
$\mathbf{e}_0$	1
$\mathbf{e}_{23}$	i
$\mathbf{e}_{31}$	j
$\mathbf{e}_{12}$	k

This correspondence can be made more precise by noting that

$$\mathbf{e}_{23} = \mathbf{I}\mathbf{e}_1, \qquad \mathbf{e}_{31} = \mathbf{I}\mathbf{e}_2, \qquad \mathbf{e}_{12} = \mathbf{I}\mathbf{e}_3, \tag{13}$$

so that (11) can be equivalently re-written as

$$q = q_0 + \mathbf{I}(q_1\mathbf{e}_1 + q_2\mathbf{e}_2 + q_3\mathbf{e}_3), \tag{14}$$

where $\bar{q} = q_1\mathbf{e}_1 + q_2\mathbf{e}_2 + q_3\mathbf{e}_3$ is a (regular) vector.

In practice, quaternions are often referred to by their scalar and vector (more precisely, bi-vector) parts as $q = (q_0, \bar{q})$, where $q_0 \in \mathbb{R}$ and $\bar{q} = [q_1, q_2, q_3]^\intercal \in \mathbb{R}^3$. Some of the properties of the quaternion algebra are summarized in Table 2. Filipe and Tsiotras[27] also conveniently defined a multiplication between real 4-by-4 matrices and quaternions, denoted by the $*$ operator, which resembles the well-known matrix-vector multiplication by simply representing the quaternion coefficients as a vector in $\mathbb{R}^4$. In other words, given $a = (a_0, \bar{a}) \in \mathbb{H}$ and a matrix $M \in \mathbb{R}^{4\times4}$ defined as

$$M = \begin{bmatrix} M_{11} & M_{12} \\ M_{21} & M_{22} \end{bmatrix}, \tag{15}$$

where $M_{11} \in \mathbb{R}$, $M_{12} \in \mathbb{R}^{1\times3}$, $M_{21} \in \mathbb{R}^{3\times1}$ and $M_{22} \in \mathbb{R}^{3\times3}$, then

$$M * a \triangleq (M_{11}a_0 + M_{12}\bar{a}, M_{21}a_0 + M_{22}\bar{a}) \in \mathbb{H}. \tag{16}$$

Table 2. Quaternion Operations

Operation	Definition
Addition	$a + b = (a_0 + b_0, \bar{a} + \bar{b})$
Scalar multiplication	$\lambda a = (\lambda a_0, \lambda a)$
Multiplication	$ab = (a_0 b_0 - \bar{a} \cdot \bar{b}, a_0 \bar{b} + b_0 \bar{a} + \bar{a} \times \bar{b})$
Conjugate	$a^* = (a_0, -\bar{a})$
Dot product	$a \cdot b = \frac{1}{2}(a^* b + b^* a)$
Cross product	$a \times b = (0, \bar{a} \times \bar{b})$
Norm	$\lVert a \rVert = \sqrt{a \cdot a}$
Scalar part	$\mathrm{sc}(a) = (a_0, 0_{3\times 1})$
Vector part	$\mathrm{vec}(a) = (0, \bar{a})$

Since any rotation can be described by three parameters, the unit norm constraint is imposed on quaternions for attitude representation. *Unit* quaternions are closed under multiplication, but not under addition. A quaternion describing the orientation of frame X with respect to frame Y, denoted by $q_{\mathrm{X/Y}}$, satisfies $q_{\mathrm{X/Y}}^* q_{\mathrm{X/Y}} = q_{\mathrm{X/Y}} q_{\mathrm{X/Y}}^* = \mathtt{1}$, where $\mathtt{1} \triangleq (1, \bar{0}_{3\times 1})$. This quaternion can be constructed as $q_{\mathrm{X/Y}} = (\cos(\phi/2), \bar{n}\sin(\theta/2))$, where $\bar{n}$ and θ are the *unit* Euler axis, and Euler angle of the rotation respectively. It is worth emphasizing that $q_{\mathrm{Y/X}}^* = q_{\mathrm{X/Y}}$, and that $q_{\mathrm{X/Y}}$ and $-q_{\mathrm{X/Y}}$ represent the same rotation. Furthermore, given quaternions $q_{\mathrm{Y/X}}$ and $q_{\mathrm{Z/Y}}$, the quaternion describing the rotation from X to Z is given by $q_{\mathrm{Z/X}} = q_{\mathrm{Y/X}} q_{\mathrm{Z/Y}}$. For completeness purposes, we define $\mathtt{0} \triangleq (0, \bar{0}_{3\times 1})$.

Three-dimensional vectors can also be interpreted as special cases of quaternions. Specifically, given $\bar{s}^{\mathrm{X}} \in \mathbb{R}^3$, the coordinates of a vector expressed in frame X, its quaternion representation is given by $s^{\mathrm{X}} = (0, \bar{s}^{\mathrm{X}}) \in \mathbb{H}^v$, where $\mathbb{H}^v$ is the set of *vector* (or *pure*) quaternions, defined as $\mathbb{H}^v \triangleq \{(q_0, \bar{q}) \in \mathbb{H} : \ q_0 = 0\}$ (see Reference 28 for further information). The change of the reference frame for a vector quaternion is achieved by the adjoint operation, and is given by $s^{\mathrm{Y}} = q_{\mathrm{Y/X}}^* s^{\mathrm{X}} q_{\mathrm{Y/X}}$. Additionally, given $s \in \mathbb{H}^v$, we can define the operation $[\,\cdot\,]^\times : \mathbb{H}^v \to \mathbb{R}^{4\times 4}$ as

$$[s]^\times = \begin{bmatrix} 0 & 0_{1\times 3} \\ 0_{3\times 1} & [\bar{s}]^\times \end{bmatrix}, \quad \text{where} \quad [\bar{s}]^\times = \begin{bmatrix} 0 & -s_3 & s_2 \\ s_3 & 0 & -s_1 \\ -s_2 & s_1 & 0 \end{bmatrix}. \tag{17}$$

For quaternions $a = (a_0, \bar{a})$ and $b = (b_0, \bar{b})$, the left and right quaternion multiplication operators $[\![\cdot]\!]_{\mathrm{L}}, [\![\cdot]\!]_{\mathrm{R}} : \mathbb{H} \to \mathbb{R}^{4\times 4}$ will be defined as

$$[\![a]\!]_{\mathrm{L}} * b \triangleq [\![b]\!]_{\mathrm{R}} * a \triangleq ab, \tag{18}$$

where

$$\llbracket a \rrbracket_{\mathrm{L}} = \left[\begin{array}{c:ccc} a_0 & -a_1 & -a_2 & -a_3 \\ \hdashline a_1 & a_0 & -a_3 & a_2 \\ a_2 & a_3 & a_0 & -a_1 \\ a_3 & -a_2 & a_1 & a_0 \end{array}\right] = \begin{bmatrix} a_0 & -\overline{a}^{\mathsf{T}} \\ \overline{a} & a_0 I_3 + [\overline{a}]^{\times} \end{bmatrix}, \tag{19}$$

$$\llbracket b \rrbracket_{\mathrm{R}} = \left[\begin{array}{c:ccc} b_0 & -b_1 & -b_2 & -b_3 \\ \hdashline b_1 & b_0 & b_3 & -b_2 \\ b_2 & -b_3 & b_0 & b_1 \\ b_3 & b_2 & -b_1 & b_0 \end{array}\right] = \begin{bmatrix} b_0 & -\overline{b}^{\mathsf{T}} \\ \overline{b} & b_0 I_3 - [\overline{b}]^{\times} \end{bmatrix}. \tag{20}$$

Quaternion Kinematics

The three-dimensional attitude kinematics in terms of unit quaternions evolve as

$$\dot{q}_{\mathrm{X/Y}} = \tfrac{1}{2} q_{\mathrm{X/Y}} \omega^{\mathrm{X}}_{\mathrm{X/Y}} = \tfrac{1}{2} \omega^{\mathrm{Y}}_{\mathrm{X/Y}} q_{\mathrm{X/Y}}, \tag{21}$$

where $\omega^{\mathrm{Z}}_{\mathrm{X/Y}} \triangleq (0, \overline{\omega}^{\mathrm{Z}}_{\mathrm{X/Y}}) \in \mathbb{H}^v$ and $\overline{\omega}^{\mathrm{Z}}_{\mathrm{X/Y}} \in \mathbb{R}^3$ is the angular velocity of frame X with respect to frame Y expressed in Z-frame coordinates.

Let I be the inertial frame of reference, B a frame fixed on the rigid body, and D the desired reference frame. The kinematic equations of motion for the B and D frames relative to the inertial frame are given, respectively, by

$$\dot{q}_{\mathrm{B/I}} = \tfrac{1}{2} q_{\mathrm{B/I}} \omega^{\mathrm{B}}_{\mathrm{B/I}}, \quad \text{and} \quad \dot{q}_{\mathrm{D/I}} = \tfrac{1}{2} q_{\mathrm{D/I}} \omega^{\mathrm{D}}_{\mathrm{D/I}}. \tag{22}$$

The attitude error kinematic equation of motion between two non-inertial frames, whose relative orientation is described by $q_{\mathrm{B/D}}$, can be easily derived to be

$$\dot{q}_{\mathrm{B/D}} = \tfrac{1}{2} q_{\mathrm{B/D}} \omega^{\mathrm{B}}_{\mathrm{B/D}}, \tag{23}$$

where $\omega^{\mathrm{B}}_{\mathrm{B/D}} = \omega^{\mathrm{B}}_{\mathrm{B/I}} - \omega^{\mathrm{B}}_{\mathrm{D/I}} = \omega^{\mathrm{B}}_{\mathrm{B/I}} - q^*_{\mathrm{B/D}} \omega^{\mathrm{D}}_{\mathrm{D/I}} q_{\mathrm{B/D}}$.

Dual Quaternions

The Clifford algebra $C\ell^+(0,3,1)(\mathbb{R}^4, Q(v))$ has the standard basis $\{1, \mathbf{e}_{23}, \mathbf{e}_{31}, \mathbf{e}_{12}, \mathbf{e}_{41}, \mathbf{e}_{42}, \mathbf{e}_{43}, \mathbf{e}_{4321}\}$, where $\mathbf{e}_1^2 = \mathbf{e}_2^2 = \mathbf{e}_3^2 = -1$ and $\mathbf{e}_4^2 = 0$. The quadratic form in this case is degenerate, and is given by $Q(v) = -v_1^2 - v_2^2 - v_3^2$, where $v = v_1\mathbf{e}_1 + v_2\mathbf{e}_2 + v_3\mathbf{e}_3 + v_4\mathbf{e}_4 \in \mathbb{R}^4$. An element of $C\ell^+(0,3,1)$ can therefore be represented as

$$\boldsymbol{q} = q_0 + q_1\mathbf{e}_{23} + q_2\mathbf{e}_{31} + q_3\mathbf{e}_{12} + q_1'\mathbf{e}_{41} + q_2'\mathbf{e}_{42} + q_3'\mathbf{e}_{43} + q_0'\mathbf{e}_{4321}, \tag{24}$$

for some real numbers $q_0, q'_0, q_1, q'_1, \ldots, q_3, q'_3$, or, equivalently,

$$\boldsymbol{q} = q_0 + q_1\mathbf{e}_{23} + q_2\mathbf{e}_{31} + q_3\mathbf{e}_{12} + \mathbf{e}_{4321}(q'_0 + q'_1\mathbf{e}_{23} + q'_2\mathbf{e}_{31} + q'_3\mathbf{e}_{12}), \tag{25}$$

where we have made use of the identities

$$\mathbf{e}_{4321}\mathbf{e}_{23} = \mathbf{e}_{41}, \qquad \mathbf{e}_{4321}\mathbf{e}_{31} = \mathbf{e}_{42}, \qquad \mathbf{e}_{4321}\mathbf{e}_{12} = \mathbf{e}_{43}. \tag{26}$$

Furthermore, notice that $\mathbf{e}_{4321}^2 = 0$.

The dual quaternion group is defined as

$$\begin{aligned} \mathbb{Q}_d := \{1, i, j, k, \epsilon, \epsilon i, \epsilon j, \epsilon k : i^2 = j^2 = k^2 = ijk = -1, \\ \epsilon i = i\epsilon, \epsilon j = j\epsilon, \epsilon k = k\epsilon, \epsilon \neq 0, \epsilon^2 = 0\}. \end{aligned} \tag{27}$$

The dual quaternion algebra arises as the algebra of the dual quaternion group $\mathbb{Q}_d$ over the field of real numbers, and is denoted as $\mathbb{H}_d$. An element in the dual quaternion algebra can therefore be expressed as

$$\begin{aligned} \boldsymbol{q} &= q_0 + q_1 i + q_2 j + q_3 k + q'_0\epsilon + q'_1\epsilon i + q'_2\epsilon j + q'_3\epsilon k \\ &= q_0 + q_1 i + q_2 j + q_3 k + \epsilon(q'_0 + q'_1 i + q'_2 j + q'_3 k). \end{aligned} \tag{28}$$

When dealing with the modeling of mechanical systems, it is convenient to define this algebra as $\mathbb{H}_d = \{\boldsymbol{q} = q_r + \epsilon q_d : q_r, q_d \in \mathbb{H}\}$, where ϵ is the dual unit. We call q_r the real (or primary) part, and q_d the dual part of the dual quaternion $\boldsymbol{q}$. Note that q_r and q_d are (regular) quaternions, combined together via the dual unit ϵ. A comparison of (25) and (28) shows immediately the similarities between this dual quaternion algebra, as originally devised by Clifford in 1873, and $C\ell^+(0,3,1)$. Specifically, Table 3 lists the matching of basis elements that establishes the isomorphism $C\ell^+(0,3,1) \cong \mathbb{H}_d$.

Table 3. Matching of Clifford algebra elements and dual quaternion algebra elements.

$C\ell^+(0,3,1)$	$\mathbb{H}_d$
$\mathbf{e}_0$	1
$\mathbf{e}_{23}$	i
$\mathbf{e}_{31}$	j
$\mathbf{e}_{12}$	k
$\mathbf{e}_{41}$	ϵi
$\mathbf{e}_{42}$	ϵj
$\mathbf{e}_{43}$	ϵk
$\mathbf{e}_{4321}$	ϵ

Filipe and Tsiotras[18,20,27,28] have laid out much of the groundwork in terms of the notation and basic properties of dual quaternions for spacecraft problems. The main properties of the dual quaternion algebra are listed in Table 4. Note that the dot product between two dual quaternions in Table 4 differs from the dot product defined in the corresponding Clifford algebra.[29] In this paper we will not make use of the dot product of two dual quaternions, only their cross product, given in Table 4.

Filipe and Tsiotras[27] also conveniently define a multiplication between matrices and dual quaternions, denoted by the $\star$ operator, that resembles the well-known real matrix-vector multiplication by simply representing the dual quaternion coefficients as a vector in $\mathbb{R}^8$. In other words, given $\boldsymbol{a} = a_r + \epsilon a_d \in \mathbb{H}_d$ and a matrix $\boldsymbol{M} \in \mathbb{R}^{8\times 8}$ defined as

$$\boldsymbol{M} = \begin{bmatrix} M_{11} & M_{12} \\ M_{21} & M_{22} \end{bmatrix}, \tag{29}$$

where $M_{11}, M_{12}, M_{21}, M_{22} \in \mathbb{R}^{4\times 4}$, then

$$\boldsymbol{M} \star \boldsymbol{a} \triangleq (M_{11} * a_r + M_{12} * a_d) + \epsilon(M_{21} * a_r + M_{22} * a_d) \in \mathbb{H}_d. \tag{30}$$

A property that arises from the definition of the circle product for dual quaternions is given by

Table 4. Dual Quaternion Operations

Operation	Definition
Addition	$\boldsymbol{a} + \boldsymbol{b} = (a_r + b_r) + \epsilon\,(a_d + b_d)$
Scalar multiplication	$\lambda\boldsymbol{a} = (\lambda a_r) + \epsilon\,(\lambda a_d)$
Multiplication	$\boldsymbol{a}\boldsymbol{b} = (a_r b_r) + \epsilon\,(a_d b_r + a_r b_d)$
Conjugate	$\boldsymbol{a}^* = (a_r^*) + \epsilon\,(a_d^*)$
Dot product	$\boldsymbol{a}\cdot\boldsymbol{b} = (a_r \cdot b_r) + \epsilon\,(a_d \cdot b_r + a_r \cdot b_d)$
Cross product	$\boldsymbol{a}\times\boldsymbol{b} = (a_r \times b_r) + \epsilon\,(a_d \times b_r + a_r \times b_d)$
Circle product	$\boldsymbol{a}\circ\boldsymbol{b} = a_r \cdot b_r + a_d \cdot b_d$
Swap	$\boldsymbol{a}^{\mathsf{s}} = a_d + \epsilon\, a_r$
Norm	$\\|\boldsymbol{a}\\| = \sqrt{\boldsymbol{a}\circ\boldsymbol{a}}$
Scalar part	$\mathrm{sc}(\boldsymbol{a}) = \mathrm{sc}(a_r) + \epsilon\,\mathrm{sc}(a_d)$
Vector part	$\mathrm{vec}(\boldsymbol{a}) = \mathrm{vec}(a_r) + \epsilon\,\mathrm{vec}(a_d)$

$$\boldsymbol{a}^{\mathsf{s}} \circ \boldsymbol{b}^{\mathsf{s}} = \boldsymbol{a}\circ\boldsymbol{b} = \boldsymbol{b}\circ\boldsymbol{a}. \tag{31}$$

Analogous to the set of vector quaternions $\mathbb{H}^v$, we can define the set of vector dual quaternions as $\mathbb{H}_d^v \triangleq \{\boldsymbol{q} = q_r + \epsilon q_d \ :\ q_r, q_d \in \mathbb{H}^v\}$. Vector dual quaternions have special properties of interest in the study of kinematics, dynamics and control of rigid bodies. The two main properties are listed below, where $\boldsymbol{a}, \boldsymbol{b} \in \mathbb{H}_d^v$:

$$\boldsymbol{a} \circ (\boldsymbol{b}\boldsymbol{c}) = \boldsymbol{b}^{\mathsf{s}} \circ (\boldsymbol{a}^{\mathsf{s}} \boldsymbol{c}^*) = \boldsymbol{c}^{\mathsf{s}} \circ (\boldsymbol{b}^* \boldsymbol{a}^{\mathsf{s}}), \tag{32}$$

$$\boldsymbol{a} \circ (\boldsymbol{b} \times \boldsymbol{c}) = \boldsymbol{b}^{\mathsf{s}} \circ (\boldsymbol{c} \times \boldsymbol{a}^{\mathsf{s}}) = \boldsymbol{c}^{\mathsf{s}} \circ (\boldsymbol{a}^{\mathsf{s}} \times \boldsymbol{b}). \tag{33}$$

For vector dual quaternions we will define the skew-symmetric operator $[\,\cdot\,]^\times : \mathbb{H}_d^v \to \mathbb{R}^{8\times 8}$,

$$[\boldsymbol{s}]^\times = \begin{bmatrix} [s_r]^\times & 0_{4\times4} \\ [s_d]^\times & [s_r]^\times \end{bmatrix}. \tag{34}$$

For dual quaternions $\boldsymbol{a} = a_r + \epsilon a_d$ and $\boldsymbol{b} = b_r + \epsilon b_d \in \mathbb{H}_d$, the left and right dual quaternion multiplication operators $[\![\,\cdot\,]\!]_{\mathrm{L}}, [\![\,\cdot\,]\!]_{\mathrm{R}} : \mathbb{H}_d \to \mathbb{R}^{8\times8}$ are defined as

$$\boldsymbol{a}\boldsymbol{b} \triangleq [\![\boldsymbol{a}]\!]_{\mathrm{L}} \star \boldsymbol{b} \triangleq [\![\boldsymbol{b}]\!]_{\mathrm{R}} \star \boldsymbol{a}, \tag{35}$$

where

$$[\![\boldsymbol{a}]\!]_{\mathrm{L}} = \begin{bmatrix} [\![a_r]\!]_{\mathrm{L}} & 0_{4\times4} \\ [\![a_d]\!]_{\mathrm{L}} & [\![a_r]\!]_{\mathrm{L}} \end{bmatrix} \quad \text{and} \quad [\![\boldsymbol{b}]\!]_{\mathrm{R}} = \begin{bmatrix} [\![b_r]\!]_{\mathrm{R}} & 0_{4\times4} \\ [\![b_d]\!]_{\mathrm{R}} & [\![b_r]\!]_{\mathrm{R}} \end{bmatrix}. \tag{36}$$

Since rigid body motion has six degrees of freedom, a dual quaternion needs two constraints to parameterize it. The dual quaternion describing the relative pose of frame B relative to I is given by $\boldsymbol{q}_{\mathrm{B/I}} = q_{\mathrm{B/I},r} + \epsilon q_{\mathrm{B/I},d} = q_{\mathrm{B/I}} + \epsilon \frac{1}{2} q_{\mathrm{B/I}} r^{\mathrm{B}}_{\mathrm{B/I}}$, where $r^{\mathrm{B}}_{\mathrm{B/I}}$ is the position quaternion describing the location of the origin of frame B relative to that of frame I, expressed in B-frame coordinates. It can be easily observed that $q_{\mathrm{B/I},r} \cdot q_{\mathrm{B/I},r} = \mathtt{1}$ and $q_{\mathrm{B/I},r} \cdot q_{\mathrm{B/I},d} = \mathtt{0}$, where $\mathtt{0} = (0, \bar{0})$, providing the two necessary constraints. Thus, a dual quaternion representing a pose transformation is a *unit* dual quaternion, since it satisfies $\boldsymbol{q} \cdot \boldsymbol{q} = \boldsymbol{q}^* \boldsymbol{q} = \mathtt{1}$, where $\mathtt{1} \triangleq \mathtt{1} + \epsilon \mathtt{0}$. Additionally, we also define $\mathtt{0} \triangleq \mathtt{0} + \epsilon \mathtt{0}$.

Similar to the standard quaternion relationships, the frame transformations laid out in Table 5 can be easily verified. In Reference 28 it was proven that for a dual unit quaternion $\boldsymbol{q} \in \mathbb{H}_d$, $\boldsymbol{q}$ and $-\boldsymbol{q}$ represent the same frame transformation,

Table 5. Unit Dual Quaternion Operations

Composition of transformations	$\boldsymbol{q}_{\mathrm{Z/X}} = \boldsymbol{q}_{\mathrm{Y/X}} \boldsymbol{q}_{\mathrm{Z/Y}}$
Inverse, Conjugate	$\boldsymbol{q}^*_{\mathrm{Y/X}} = \boldsymbol{q}_{\mathrm{X/Y}}$

property inherited from the space of quaternions. Therefore, as is done in practice for quaternions, dual quaternions can be subjected to properization, which is the action of redefining a dual quaternion so that the scalar part of the quaternion is always positive. Formally, we can define the properization of a dual quaternion $\boldsymbol{q} = q_r + \epsilon q_d$ as

$$\boldsymbol{q} \coloneqq -\boldsymbol{q} \quad \text{if} \quad (q_r)_0 < 0, \tag{37}$$

where $(q_r)_0$ is the scalar part of q_r.

Dual Quaternion Kinematics

The dual velocity of the Y-frame with respect to the Z-frame, expressed in X-frame coordinates, is defined as

$$\boldsymbol{\omega}^{\mathrm{X}}_{\mathrm{Y/Z}} = \boldsymbol{q}^*_{\mathrm{X/Y}} \boldsymbol{\omega}^{\mathrm{Y}}_{\mathrm{Y/Z}} \boldsymbol{q}_{\mathrm{X/Y}} = \omega^{\mathrm{X}}_{\mathrm{Y/Z}} + \epsilon(v^{\mathrm{X}}_{\mathrm{Y/Z}} + \omega^{\mathrm{X}}_{\mathrm{Y/Z}} \times r^{\mathrm{X}}_{\mathrm{X/Y}}), \tag{38}$$

where $\omega^{\mathrm{X}}_{\mathrm{Y/Z}} = (0, \bar{\omega}^{\mathrm{X}}_{\mathrm{Y/Z}})$ and $v^{\mathrm{X}}_{\mathrm{Y/Z}} = (0, \bar{v}^{\mathrm{X}}_{\mathrm{Y/Z}})$, $\bar{\omega}^{\mathrm{X}}_{\mathrm{Y/Z}}$ and $\bar{v}^{\mathrm{X}}_{\mathrm{Y/Z}} \in \mathbb{R}^3$ are respectively the angular and linear velocity of the Y-frame with respect to the Z-frame expressed in X-frame coordinates, and $r^{\mathrm{X}}_{\mathrm{X/Y}} = (0, \bar{r}^{\mathrm{X}}_{\mathrm{X/Y}})$, where $\bar{r}^{\mathrm{X}}_{\mathrm{X/Y}} \in \mathbb{R}^3$ is the position vector from the origin of the Y-frame to the origin of the X-frame expressed in X-frame coordinates. In particular, from equation (38) we observe that the dual velocity of a rigid body assigned to frame B with respect to the inertial frame, expressed in B-frame coordinates is given as $\boldsymbol{\omega}^{\mathrm{B}}_{\mathrm{B/I}} = \omega^{\mathrm{B}}_{\mathrm{B/I}} + \epsilon v^{\mathrm{B}}_{\mathrm{B/I}}$.

In general, the dual quaternion kinematics can be expressed as[27]

$$\dot{\boldsymbol{q}}_{\mathrm{X/Y}} = \tfrac{1}{2} \boldsymbol{q}_{\mathrm{X/Y}} \boldsymbol{\omega}^{\mathrm{X}}_{\mathrm{X/Y}} = \tfrac{1}{2} \boldsymbol{\omega}^{\mathrm{Y}}_{\mathrm{X/Y}} \boldsymbol{q}_{\mathrm{X/Y}}. \tag{39}$$

One of the key advantages of dual quaternions is the resemblance, in form, of the *pose* error kinematic equations of motion to the attitude-only error kinematics. The pose error kinematic equation of motion between non-inertial frames B and D, is given by

$$\dot{\boldsymbol{q}}_{\mathrm{B/D}} = \tfrac{1}{2} \boldsymbol{q}_{\mathrm{B/D}} \boldsymbol{\omega}^{\mathrm{B}}_{\mathrm{B/D}}, \tag{40}$$

where $\boldsymbol{\omega}^{\mathrm{B}}_{\mathrm{B/D}} = \boldsymbol{\omega}^{\mathrm{B}}_{\mathrm{B/I}} - \boldsymbol{\omega}^{\mathrm{B}}_{\mathrm{D/I}} = \boldsymbol{\omega}^{\mathrm{B}}_{\mathrm{B/I}} - \boldsymbol{q}^*_{\mathrm{B/D}} \boldsymbol{\omega}^{\mathrm{D}}_{\mathrm{D/I}} \boldsymbol{q}_{\mathrm{B/D}}$. It is worth comparing at this point (40) with (23).

Dynamics

The rotational(-only) Euler equation of motion expressed in terms of quaternions is

$$I^{\mathrm{B}} * \dot{\omega}^{\mathrm{B}}_{\mathrm{B/I}} + \omega^{\mathrm{B}}_{\mathrm{B/I}} \times I^{\mathrm{B}} * \omega^{\mathrm{B}}_{\mathrm{B/I}} = \tau^{\mathrm{B}}, \tag{41}$$

where $I^{\mathrm{B}} = \mathrm{diag}(1, \bar{I}^{\mathrm{B}})$, and $\tau^{\mathrm{B}} \in \mathbb{H}^v$ is the net external moment about the center of mass. Defining the *dual inertia matrix* for a rigid body as[27]

$$M^{\mathrm{B}} \triangleq \begin{bmatrix} 1 & 0_{1\times 3} & 0 & 0_{1\times 3} \\ 0_{3\times 1} & m\,\mathbb{I}_3 & 0_{3\times 1} & 0_{3\times 3} \\ 0 & 0_{1\times 3} & 1 & 0_{1\times 3} \\ 0_{3\times 1} & 0_{3\times 3} & 0_{3\times 1} & \bar{I}^{\mathrm{B}} \end{bmatrix}, \tag{42}$$

where $m > 0$ is the mass of the rigid body, $\bar{I}^{\mathrm{B}} \in \mathbb{R}^{3\times 3}$ is the inertia matrix computed in B-frame coordinates about the center of mass, and $\mathbb{I}_3$ is the 3-by-3 identity matrix. Then, the Newton-Euler equations of motion for a rigid body in 6-DOF motion are given in terms of dual quaternions as

$$M^{\mathrm{B}} \star (\dot{\boldsymbol{\omega}}^{\mathrm{B}}_{\mathrm{B/I}})^{\mathsf{s}} + \boldsymbol{\omega}^{\mathrm{B}}_{\mathrm{B/I}} \times \left(M^{\mathrm{B}} \star (\boldsymbol{\omega}^{\mathrm{B}}_{\mathrm{B/I}})^{\mathsf{s}}\right) = \boldsymbol{f}^{\mathrm{B}}, \tag{43}$$

where $\boldsymbol{f}^{\mathrm{B}} = f^{\mathrm{B}} + \epsilon\tau^{\mathrm{B}}$ is the dual force applied on the body about its center of mass. Again, it is worth comparing the similarity between (43) and (41).

The attitude(-only) error dynamic equations of motion for a rigid body are given by

$$I^{\mathrm{B}} * \dot{\omega}^{\mathrm{B}}_{\mathrm{B/D}} = \tau^{\mathrm{B}} - (\omega^{\mathrm{B}}_{\mathrm{B/D}} + \omega^{\mathrm{B}}_{\mathrm{D/I}}) \times \left(I^{\mathrm{B}} * (\omega^{\mathrm{B}}_{\mathrm{B/D}} + \omega^{\mathrm{B}}_{\mathrm{D/I}})\right) - I^{\mathrm{B}} * (q^*_{\mathrm{B/D}} \dot{\omega}^{\mathrm{D}}_{\mathrm{D/I}} q_{\mathrm{B/D}}) - I^{\mathrm{B}} * (\omega^{\mathrm{B}}_{\mathrm{D/I}} \times \omega^{\mathrm{B}}_{\mathrm{B/D}}). \tag{44}$$

Equation (44) describes the time-evolution of the angular velocity of a frame fixed to a rigid body B relative to a desired reference frame D, both of which are evolving with respect to the inertial frame I. In Reference 27, the authors provide the *pose* error dynamics in a manner that closely resembles the attitude(-only) error dynamic equations of motion. The pose error dynamics can be derived by substituting the expression $\boldsymbol{\omega}^{\mathrm{B}}_{\mathrm{B/I}} = \boldsymbol{\omega}^{\mathrm{B}}_{\mathrm{B/D}} + \boldsymbol{\omega}^{\mathrm{B}}_{\mathrm{D/I}} = \boldsymbol{\omega}^{\mathrm{B}}_{\mathrm{B/D}} + \boldsymbol{q}^*_{\mathrm{B/D}} \boldsymbol{\omega}^{\mathrm{D}}_{\mathrm{D/I}} \boldsymbol{q}_{\mathrm{B/D}}$ into equation (43) to yield

$$M^{\mathrm{B}} \star (\dot{\boldsymbol{\omega}}^{\mathrm{B}}_{\mathrm{B/D}})^{\mathsf{s}} = \boldsymbol{f}^{\mathrm{B}} - (\boldsymbol{\omega}^{\mathrm{B}}_{\mathrm{B/D}} + \boldsymbol{\omega}^{\mathrm{B}}_{\mathrm{D/I}}) \times \left(M^{\mathrm{B}} \star ((\boldsymbol{\omega}^{\mathrm{B}}_{\mathrm{B/D}})^{\mathsf{s}} + (\boldsymbol{\omega}^{\mathrm{B}}_{\mathrm{D/I}})^{\mathsf{s}})\right) - M^{\mathrm{B}} \star (\boldsymbol{q}^*_{\mathrm{B/D}} \dot{\boldsymbol{\omega}}^{\mathrm{D}}_{\mathrm{D/I}} \boldsymbol{q}_{\mathrm{B/D}})^{\mathsf{s}} - M^{\mathrm{B}} \star (\boldsymbol{\omega}^{\mathrm{B}}_{\mathrm{D/I}} \times \boldsymbol{\omega}^{\mathrm{B}}_{\mathrm{B/D}})^{\mathsf{s}}. \tag{45}$$

It is immediately seen that equation (41) and equation (43) have the same structure, as do equation (44) and equation (45). This characteristic can be exploited for control design of 6-DOF systems based on existing 3-DOF controllers.

Next, we provide a typical decomposition of $\boldsymbol{f}^{\mathrm{B}}$, the total external dual force acting on an Earth-orbiting spacecraft. Without loss of generality, $\boldsymbol{f}^{\mathrm{B}}$ can be described as follows:[28]

$$\boldsymbol{f}^{\mathrm{B}} = \boldsymbol{f}^{\mathrm{B}}_g + \boldsymbol{f}^{\mathrm{B}}_{\nabla g} + \boldsymbol{f}^{\mathrm{B}}_{J_2} + \boldsymbol{f}^{\mathrm{B}}_d + \boldsymbol{f}^{\mathrm{B}}_c, \tag{46}$$

where $\boldsymbol{f}^{\mathrm{B}}_g$ is the dual gravitational force, $\boldsymbol{f}^{\mathrm{B}}_{\nabla g}$ is the dual gravity gradient force, $\boldsymbol{f}^{\mathrm{B}}_{J_2}$ is the dual perturbing force due to Earth's oblateness, $\boldsymbol{f}_d^{\mathrm{B}}$ is a dual disturbance force, and $\boldsymbol{f}_c^{\mathrm{B}}$ is the dual control force. In application, the dual control force is calculated as $\boldsymbol{f}_c^{\mathrm{B}} = \boldsymbol{f}^{\mathrm{B}} - \boldsymbol{f}_g^{\mathrm{B}} - \boldsymbol{f}_{\nabla g}^{\mathrm{B}} - \boldsymbol{f}_{J_2}^{\mathrm{B}} - \boldsymbol{f}_d^{\mathrm{B}}$, where $\boldsymbol{f}^{\mathrm{B}}$ is usually the variable designed in pose controllers. For the sake of completeness, we provide common expressions for the gravitational terms and the J_2 term.

The dual gravitational force can be described as $\boldsymbol{f}_g^{\mathrm{B}} = m\boldsymbol{a}_g^{\mathrm{B}}, \boldsymbol{a}_g^{\mathrm{B}} = a_g^{\mathrm{B}} + \epsilon 0$, $a_g^{\mathrm{B}} = (0, \bar{a}_g^{\mathrm{B}})$, where $\bar{a}_g^{\mathrm{B}} \in \mathbb{R}^3$ is the gravitational acceleration given by

$$\bar{a}_g^{\mathrm{B}} = -\mu \frac{\bar{r}_{\mathrm{B/I}}^{\mathrm{B}}}{\|\bar{r}_{\mathrm{B/I}}^{\mathrm{B}}\|^3}, \tag{47}$$

$\mu = 398600.4418$ km^3/s^2 is Earth's gravitational parameter.

The dual gravity gradient force can be described as $\boldsymbol{f}_{\nabla g}^{\mathrm{B}} = 0 + \epsilon \tau_{\nabla g}^{\mathrm{B}}$, $\tau_{\nabla g}^{\mathrm{B}} = (0, \bar{\tau}_{\nabla g}^{\mathrm{B}})$, where $\bar{\tau}_{\nabla g}^{\mathrm{B}} \in \mathbb{R}^3$ is the gravity gradient torque, which can be written as

$$\bar{\tau}_{\nabla g}^{\mathrm{B}} = 3\mu \frac{\bar{r}_{\mathrm{B/I}}^{\mathrm{B}} \times (\bar{I}^{\mathrm{B}} \bar{r}_{\mathrm{B/I}}^{\mathrm{B}})}{\|\bar{r}_{\mathrm{B/I}}^{\mathrm{B}}\|^5}. \tag{48}$$

The dual perturbing force due to Earth's oblateness can be described as $\boldsymbol{f}_{J_2}^{\mathrm{B}} = m\boldsymbol{a}_{J_2}^{\mathrm{B}}, \boldsymbol{a}_{J_2}^{\mathrm{B}} = a_{J_2}^{\mathrm{B}} + \epsilon 0$, $a_{J_2}^{\mathrm{B}} = (0, \bar{a}_{J_2}^{\mathrm{B}})$, where $\bar{a}_{J_2}^{\mathrm{B}} \in \mathbb{R}^3$ is the perturbing acceleration due to J_2. This acceleration can be computed in inertial frame coordinates as

$$\bar{a}_{J_2}^{\mathrm{I}} = -\frac{3}{2} \frac{\mu J_2 R_e^2}{\|\bar{r}_{\mathrm{B/I}}^{\mathrm{I}}\|^5} \begin{bmatrix} (1 - 5c^2)\, x_{\mathrm{B/I}}^{\mathrm{I}} \\ (1 - 5c^2)\, y_{\mathrm{B/I}}^{\mathrm{I}} \\ (3 - 5c^2)\, z_{\mathrm{B/I}}^{\mathrm{I}} \end{bmatrix}, \tag{49}$$

where $c = z_{\mathrm{B/I}}^{\mathrm{I}} / \|\bar{r}_{\mathrm{B/I}}^{\mathrm{I}}\|$, $J_2 = 0.0010826267$ and $R_e = 6378.137$ km is Earth's mean equatorial radius.

The expressions for the gravitational dual force, the gravity gradient dual force, and perturbations due to J_2 are provided in terms of the dual inertia matrix as:[28]

$$\boldsymbol{f}_g^{\mathrm{B}} = M^{\mathrm{B}} \star \boldsymbol{a}_g^{\mathrm{B}}, \tag{50}$$

$$\boldsymbol{f}_{J_2}^{\mathrm{B}} = M^{\mathrm{B}} \star \boldsymbol{a}_{J_2}^{\mathrm{B}}, \tag{51}$$

We propose re-defining the gravity gradient dual force as

$$\boldsymbol{f}_{\nabla g}^{\mathrm{B}} = \frac{3\mu (\boldsymbol{r}_{\mathrm{B/I}}^{\mathrm{B}})^{\mathsf{s}}}{\|\boldsymbol{r}_{\mathrm{B/I}}^{\mathrm{B}}\|^5} \times (M^{\mathrm{B}} \star \boldsymbol{r}_{\mathrm{B/I}}^{\mathrm{B}}), \quad \boldsymbol{r}_{\mathrm{B/I}}^{\mathrm{B}} \triangleq 0 + \epsilon r_{\mathrm{B/I}}^{\mathrm{B}}, \tag{52}$$

which uses the appropriate native representation of a position vector expressed in dual quaternion algebra.[30] In summary, we can represent $\boldsymbol{f}^{\mathrm{B}}$ as

$$\boldsymbol{f}^{\mathrm{B}} = \boldsymbol{f}_g^{\mathrm{B}} + \boldsymbol{f}_{\nabla g}^{\mathrm{B}} + \boldsymbol{f}_{J_2}^{\mathrm{B}} + \boldsymbol{f}_d^{\mathrm{B}} + \boldsymbol{f}_c^{\mathrm{B}} = M^{\mathrm{B}} \star \boldsymbol{a}_g^{\mathrm{B}} + \frac{3\mu (\boldsymbol{r}_{\mathrm{B/I}}^{\mathrm{B}})^{\mathsf{s}}}{\|\boldsymbol{r}_{\mathrm{B/I}}^{\mathrm{B}}\|^5} \times (M^{\mathrm{B}} \star \boldsymbol{r}_{\mathrm{B/I}}^{\mathrm{B}}) + M^{\mathrm{B}} \star \boldsymbol{a}_{J_2}^{\mathrm{B}} + \boldsymbol{f}_d^{\mathrm{B}} + \boldsymbol{f}_c^{\mathrm{B}} \tag{53}$$

DUAL QUATERNIONS FOR SPACECRAFT POSE ESTIMATION AND CONTROL

Dual quaternions have been found to be particularly useful in cases when spacecraft position – in addition to its attitude – needs to be controlled or estimated. In particular, previous work by Filipe and Tsiotras[18–20,27,31] exploited the algebraic similarities between quaternion and dual quaternion algebras to extend attitude-only results to position-and-attitude (pose) results. For example, the attitude stabilizing law

$$\tau^{\mathrm{B}} = -k_p \mathrm{vec}\big(q_{\mathrm{B/I}}\big) - k_d \omega^{\mathrm{B}}_{\mathrm{B/I}}, \tag{54}$$

which establishes (almost) global asymptotic stability for the attitude of a rigid body, was extended to the pose stabilizing control law in terms of dual quaternions[27]

$$\boldsymbol{f}^{\mathrm{B}} = -k_p \mathrm{vec}\big(\boldsymbol{q}^*_{\mathrm{B/I}}(\boldsymbol{q}_{\mathrm{B/I}} - \mathtt{1})^{\mathsf{s}}\big) - k_d(\boldsymbol{\omega}^{\mathrm{B}}_{\mathrm{B/I}})^{\mathsf{s}}, \tag{55}$$

which yields (almost) global asymptotic stability for the pose of a rigid body.

Lizarralde and Wen used passivity to stabilize the attitude of a spacecraft using the control law[32]

$$\tau^{\mathrm{B}} = -k_p \mathrm{vec}\big(q_{\mathrm{B/D}}\big) - 2\mathrm{vec}\big(q^*_{\mathrm{B/D}} z\big), \tag{56}$$

where z is the output of an LTI system of the form

$$\begin{aligned} \dot{x}_{\mathrm{p}} &= A * x_{\mathrm{p}} + B * q_{\mathrm{B/D}} \\ z &= (CA) * x_{\mathrm{p}} + (CB) * q_{\mathrm{B/D}}. \end{aligned} \tag{57}$$

This result was extended to a dual quaternion stabilization controller given by[27]

$$\boldsymbol{f}^{\mathrm{B}} = -k_p \mathrm{vec}\big(\boldsymbol{q}^*_{\mathrm{B/D}}(\boldsymbol{q}^{\mathsf{s}}_{\mathrm{B/D}} - \mathtt{1}^{\mathsf{s}})\big) - 2\mathrm{vec}\big(\boldsymbol{q}^*_{\mathrm{B/D}} \boldsymbol{z}^{\mathsf{s}}\big), \tag{58}$$

where $\boldsymbol{z}$ is the output of an LTI system of the form

$$\begin{aligned} \dot{\boldsymbol{x}}_{\mathrm{p}} &= A \star \boldsymbol{x}_{\mathrm{p}} + B \star \boldsymbol{q}_{\mathrm{B/D}} \\ \boldsymbol{z} &= (CA) \star \boldsymbol{x}_{\mathrm{p}} + (CB) \star \boldsymbol{q}_{\mathrm{B/D}}. \end{aligned} \tag{59}$$

This parallelism between attitude and pose controllers was further elaborated for model-based (known inertia-matrix) reference tracking. The control law by Wen and Kreutz-Delgado[33]

$$\tau^{\mathrm{B}} = -k_p \mathrm{vec}\big(q_{\mathrm{B/D}}\big) - k_d \omega^{\mathrm{B}}_{\mathrm{B/D}} + I^{\mathrm{B}} * (q^*_{\mathrm{B/D}} \dot{\omega}^{\mathrm{D}}_{\mathrm{D/I}} q_{\mathrm{B/D}}) + \omega^{\mathrm{B}}_{\mathrm{D/I}} \times (I^{\mathrm{B}} * \omega^{\mathrm{B}}_{\mathrm{D/I}}) \tag{60}$$

yields (almost) global asymptotic stability of the attitude of a spacecraft during tracking of a time-dependent reference. This control law was extended to a pose-tracking controller in terms of dual quaternions resulting in[21]

$$\boldsymbol{f}^{\mathrm{B}} = -\, k_p \mathrm{vec}\big(\boldsymbol{q}^*_{\mathrm{B/D}}(\boldsymbol{q}^{\mathsf{s}}_{\mathrm{B/D}} - 1^{\mathsf{s}})\big) - k_d (\boldsymbol{\omega}^{\mathrm{B}}_{\mathrm{B/D}})^{\mathsf{s}} + M^{\mathrm{B}} \star (\boldsymbol{q}^*_{\mathrm{B/D}} \dot{\boldsymbol{\omega}}^{\mathrm{D}}_{\mathrm{D/I}} \boldsymbol{q}_{\mathrm{B/D}})^{\mathsf{s}} + \boldsymbol{\omega}^{\mathrm{B}}_{\mathrm{D/I}} \times (M^{\mathrm{B}} \star (\boldsymbol{\omega}^{\mathrm{B}}_{\mathrm{D/I}})^{\mathsf{s}}). \tag{61}$$

The need for dual velocity feedback was lifted during tracking maneuvers, yielding the controller[18,21]

$$\boldsymbol{f}^{\mathrm{B}} = -k_p \mathrm{vec}\big(\boldsymbol{q}^*_{\mathrm{B/D}}(\boldsymbol{q}^{\mathsf{s}}_{\mathrm{B/D}} - 1^{\mathsf{s}})\big) - 2\mathrm{vec}\big(\boldsymbol{q}^*_{\mathrm{B/D}} \boldsymbol{z}^{\mathsf{s}}\big) + M^{\mathrm{B}} \star (\boldsymbol{q}^*_{\mathrm{B/D}} \dot{\boldsymbol{\omega}}^{\mathrm{D}}_{\mathrm{D/I}} \boldsymbol{q}_{\mathrm{B/D}})^{\mathsf{s}} + \boldsymbol{\omega}^{\mathrm{B}}_{\mathrm{D/I}} \times (M^{\mathrm{B}} \star (\boldsymbol{\omega}^{\mathrm{B}}_{\mathrm{D/I}})^{\mathsf{s}}), \tag{62}$$

where $\boldsymbol{z}$ is the output of the same LTI system given in equation (57).

Moreover, a result which cements the importance of dual quaternions for rigid-body control is the extension of the attitude(-only) controller given as[34]

$$\begin{aligned}\tau^{\mathrm{B}} = &-\mathrm{vec}\big(q_{\mathrm{B/D}}\big) - K_\omega * \omega^{\mathrm{B}}_{\mathrm{B/D}} - (K_\omega K_q) * q_{\mathrm{B/D}} + \omega^{\mathrm{B}}_{\mathrm{B/I}} \times (\widehat{I}^{\mathrm{B}} * \omega^{\mathrm{B}}_{\mathrm{B/I}}) + \widehat{I}^{\mathrm{B}} * (q^*_{\mathrm{B/D}} \dot{\omega}^{\mathrm{D}}_{\mathrm{D/I}} q_{\mathrm{B/D}}) \\ &+ \widehat{I}^{\mathrm{B}} * (\omega^{\mathrm{B}}_{\mathrm{D/I}} \times \omega^{\mathrm{B}}_{\mathrm{B/D}}) - (\widehat{I}^{\mathrm{B}} K_q) * \frac{\mathrm{d}}{\mathrm{d}t}(q_{\mathrm{B/D}}),\end{aligned} \tag{63}$$

where $\widehat{I}^{\mathrm{B}}$ is an adaptive estimate of the inertia matrix. Equation (63) is a model-free attitude-tracking controller which under the right conditions ensures inertia matrix identification. The controller in equation (63) was extended to a 6-DOF spacecraft pose-tracking controller in Reference 20 (with the appropriate corrections incorporated in Reference 28), given as

$$\begin{aligned}\boldsymbol{f}^{\mathrm{B}}_c = &-\widehat{M^{\mathrm{B}}} \star \boldsymbol{a}^{\mathrm{B}}_g - \frac{3\mu \boldsymbol{r}^{\mathrm{B}}_{\mathrm{B/I}}}{\|\boldsymbol{r}^{\mathrm{B}}_{\mathrm{B/I}}\|^5} \times (\widehat{M^{\mathrm{B}}} \star (\boldsymbol{r}^{\mathrm{B}}_{\mathrm{B/I}})^{\mathsf{s}}) - \widehat{M^{\mathrm{B}}} \star \boldsymbol{a}^{\mathrm{B}}_{J_2} - \widehat{\boldsymbol{f}}^{\mathrm{B}}_d \\ &-\mathrm{vec}\big(\boldsymbol{q}^*_{\mathrm{B/D}}(\boldsymbol{q}^{\mathsf{s}}_{\mathrm{B/D}} - 1^{\mathsf{s}})\big) - K_d \star \boldsymbol{s}^{\mathsf{s}} + \boldsymbol{\omega}^{\mathrm{B}}_{\mathrm{B/I}} \times (\widehat{M^{\mathrm{B}}} \star (\boldsymbol{\omega}^{\mathrm{B}}_{\mathrm{B/I}})^{\mathsf{s}}) + \widehat{M^{\mathrm{B}}} \star (\boldsymbol{q}^*_{\mathrm{B/D}} \dot{\boldsymbol{\omega}}^{\mathrm{D}}_{\mathrm{D/I}} \boldsymbol{q}_{\mathrm{B/D}})^{\mathsf{s}} \\ &+ \widehat{M^{\mathrm{B}}} \star (\boldsymbol{\omega}^{\mathrm{B}}_{\mathrm{D/I}} \times \boldsymbol{\omega}^{\mathrm{B}}_{\mathrm{B/D}})^{\mathsf{s}} - \widehat{M^{\mathrm{B}}} \star (K_p \star \frac{\mathrm{d}}{\mathrm{d}t}(\boldsymbol{q}^*_{\mathrm{B/D}}(\boldsymbol{q}^{\mathsf{s}}_{\mathrm{B/D}} - 1^{\mathsf{s}}))),\end{aligned} \tag{64}$$

where $\widehat{M^{\mathrm{B}}}$ is an adaptive estimate of the dual inertia matrix. Up to the terms associated to the gravitational field, the dual part of the control law given by equation (64) is identical to equation (63). As expected, under the right conditions, the controller proposed in Reference 20 will ensure dual inertia matrix identification.

Dual quaternions have also been successfully used for pose estimation. Again, by exploiting the similarities between quaternion and dual quaternion algebra, the landmark Multiplicative Extended Kalman Filter for attitude estimation first derived by Lefferts et al.[35] was extended to include position estimates in the form of a Dual Quaternion Multiplicative Extended Kalman Filter (DQ-MEKF).[36,37]

The DQ-MEKF is a continuous-discrete EKF that takes continuous-time angular velocity and linear acceleration measurements with noise and bias from the rate-gyros and the IMU, respectively, and discrete-time pose measurements with noise.[36] The state and process noise vectors are

$$x = \begin{bmatrix} \overline{\delta \boldsymbol{q}_{\text{B/I}}}^{\mathsf{T}} & \overline{\boldsymbol{b}_{\boldsymbol{\omega}}}^{\mathsf{T}} & \overline{b}_n^{\mathsf{T}} \end{bmatrix}^{\mathsf{T}} \in \mathbb{R}^{15} \quad \text{and} \quad w = \begin{bmatrix} \overline{\boldsymbol{\eta}_{\boldsymbol{\omega}}}^{\mathsf{T}} & \overline{\eta}_{b_\omega}^{\mathsf{T}} & \overline{\eta}_n^{\mathsf{T}} & \overline{\eta}_{b_n}^{\mathsf{T}} \end{bmatrix}^{\mathsf{T}} \in \mathbb{R}^{15}, \tag{65}$$

where $\delta \boldsymbol{q}_{\text{B/I}} = \hat{\boldsymbol{q}}_{\text{B/I}}^* \boldsymbol{q}_{\text{B/I}}$ is the dual error quaternion between the current best guess $\hat{\boldsymbol{q}}_{\text{B/I}}$ and the true dual quaternion $\boldsymbol{q}_{\text{B/I}}$, $\overline{\delta \boldsymbol{q}_{\text{B/I}}} \in \mathbb{R}^6$ is the vector part of the dual quaternion $\delta \boldsymbol{q}_{\text{B/I}}$, $\boldsymbol{b}_{\boldsymbol{\omega}} = b_\omega + \epsilon b_v$ is the dual bias, $b_\omega = (0, \overline{b}_\omega)$, $\overline{b}_\omega \in \mathbb{R}^3$ is the bias of the angular velocity measurement, $b_v = (0, \overline{b}_v)$, $\overline{b}_v \in \mathbb{R}^3$ is the bias of the linear velocity measurement, $b_n = (0, \overline{b}_n)$, and $\overline{b}_n \in \mathbb{R}^3$ is the bias of the specific force measurement. Also, $\boldsymbol{\eta}_{\boldsymbol{\omega}} = \eta_\omega + \epsilon \eta_v$, $\eta_\omega = (0, \overline{\eta}_\omega)$, $\overline{\eta}_\omega \in \mathbb{R}^3$ is the noise of the angular velocity measurements assumed to be a zero-mean Gaussian white noise process, $\eta_v = (0, \overline{\eta}_v)$, $\overline{\eta}_v \in \mathbb{R}^3$ is the noise of the linear velocity measurements assumed to be a zero-mean Gaussian white noise process, $\overline{\eta}_n \in \mathbb{R}^3$ is the noise of the specific force measurement assumed to be a Gaussian white noise process, and $\overline{\eta}_{b_\omega} \in \mathbb{R}^3$ and $\overline{\eta}_{b_n} \in \mathbb{R}^3$ are also zero-mean Gaussian white noise processes that drive the corresponding biases by $\dot{\overline{b}}_\omega = \overline{\eta}_{b_\omega}$ and $\dot{\overline{b}}_n = \overline{\eta}_{b_n}$ respectively.

The general form of the non-linear output is $z_m(t_k) = h_m(x_n(t_k)) + v_m(t_k)$. The specific form used for the DQ-MEKF implementation used in Reference 38 is given by

$$\overline{(\hat{\boldsymbol{q}}_{\text{B/I}}^-(t_k))^* \boldsymbol{q}_{\text{B/I},m}(t_k)} = \overline{\delta \boldsymbol{q}_{\text{B/I}}(t_k)} + v(t_k), \tag{66}$$

where $z(t_k) = \overline{(\hat{\boldsymbol{q}}_{\text{B/I}}^-(t_k))^* \boldsymbol{q}_{\text{B/I},m}(t_k)}$ and $h(x(t_k)) = \overline{\delta \boldsymbol{q}_{\text{B/I}}(t_k)}$. Moreover, with the optimal Kalman state update calculated by

$$\Delta^\star \hat{x}(t_k) \triangleq \begin{bmatrix} \Delta^\star \overline{\delta \hat{\boldsymbol{q}}_{\text{B/I}}}(t_k) \\ \Delta^\star \hat{\overline{\boldsymbol{b}}}_{\boldsymbol{\omega}}(t_k) \\ \Delta^\star \hat{\overline{b}}_n(t_k) \end{bmatrix} = K(t_k)(z(t_k) - \hat{z}(t_k)) = K(t_k)\overline{(\hat{\boldsymbol{q}}_{\text{B/I}}^-(t_k))^* \boldsymbol{q}_{\text{B/I},m}(t_k)}, \tag{67}$$

and $\Delta^\star \delta \hat{\boldsymbol{q}}_{\text{B/I}}$ reconstructed as[28]

$$\Delta^\star \delta \hat{\boldsymbol{q}}_{\text{B/I}} = \left(\sqrt{1 - \|\Delta^\star \overline{\delta \hat{q}_{\text{B/I},r}}\|^2}, \Delta^\star \overline{\delta \hat{q}_{\text{B/I},r}} \right) + \epsilon \left(\frac{-\Delta^\star \overline{\delta \hat{q}_{\text{B/I},r}}^{\mathsf{T}} \Delta^\star \overline{\delta \hat{q}_{\text{B/I},d}}}{\sqrt{1 - \|\Delta^\star \overline{\delta \hat{q}_{\text{B/I},r}}\|^2}}, \Delta^\star \overline{\delta \hat{q}_{\text{B/I},d}} \right), \tag{68}$$

the estimate of the state at time t_k after a measurement is calculated from

$$\hat{\boldsymbol{q}}^{+}_{\text{B/I}}(t_k) = \hat{\boldsymbol{q}}^{-}_{\text{B/I}}(t_k)\Delta^{\star}\delta\hat{\boldsymbol{q}}_{\text{B/I}}(t_k), \tag{69}$$

$$\overline{\hat{\boldsymbol{b}}}^{+}_{\boldsymbol{\omega}}(t_k) = \overline{\hat{\boldsymbol{b}}}^{-}_{\boldsymbol{\omega}}(t_k) + \Delta^{\star}\overline{\hat{\boldsymbol{b}}}_{\boldsymbol{\omega}}(t_k), \tag{70}$$

$$\overline{\hat{b}}^{+}_{n}(t_k) = \overline{\hat{b}}^{-}_{n}(t_k) + \Delta^{\star}\overline{\hat{b}}_{n}(t_k), \tag{71}$$

and $K(t_k) \in \mathbb{R}^{15\times 6}$. We refer the reader to Reference 36 for a detailed derivation of the DQ-MEKF.

Other important dual quaternion results address the issue of robustness,[14] and the issue of the unwinding phenomenon,[39] which dual quaternions inherit from quaternions, using hybrid systems theory. The result in Reference 22 provides a 6-DOF controller based on the non-certainty equivalence principle. Additional dual quaternion-based estimators include those in Reference 40 and Reference 41, which use twistors for the implementation of an Unscented Kalman Filter. All these results share the ability of estimating pose – in particular *relative* pose with respect to another spacecraft – making them useful during spacecraft proximity operations as has been demonstrated experimentally.[28,38]

POSE-TRACKING ADAPTIVE CONTROLLER USING CONTINUOUS CONCURRENT LEARNING

Concurrent Learning

Concurrent learning is a recently proposed approach that makes use of the current measured state of the system, and possibly previously recorded data, to modify the adaptation of the unknown parameters in an adaptive control setting. Section 3 of Reference 42 lays out the fundamental results for the theory. An overview of how the concept feeds into Lyapunov stability theory is provided here for the reader's convenience, in the context of the estimation of the mass properties for a spacecraft.

The first step is to recast the dynamics from equation (45) in a way that is amenable to the concurrent learning framework. To this end, define $\mathrm{v}(M^{\text{B}}) = [I_{11}\ I_{12}\ I_{13}\ I_{22}\ I_{23}\ I_{33}\ m]^{\mathsf{T}} \in \mathbb{R}^7$ to be the vectorized version of the dual inertia matrix M^{B}. Also, let the error in the estimation of the dual inertia matrix be

$$\Delta M^{\text{B}} = \widehat{M^{\text{B}}} - M^{\text{B}}, \tag{72}$$

as originally defined in Reference 19. This allows us to define the auxiliary function $r : \mathbb{H}_d^v \to \mathbb{R}^{8\times 7}$ that satisfies

$$M^{\text{B}} \star \boldsymbol{a} \triangleq r(\boldsymbol{a})\mathrm{v}(M^{\text{B}}) = \begin{bmatrix} 0 & 0 & 0 & 0 & 0 & 0 & 0 \\ 0 & 0 & 0 & 0 & 0 & 0 & a_2 \\ 0 & 0 & 0 & 0 & 0 & 0 & a_3 \\ 0 & 0 & 0 & 0 & 0 & 0 & a_4 \\ 0 & 0 & 0 & 0 & 0 & 0 & 0 \\ a_6 & a_7 & a_8 & 0 & 0 & 0 & 0 \\ 0 & a_6 & 0 & a_7 & a_8 & 0 & 0 \\ 0 & 0 & a_6 & 0 & a_7 & a_8 & 0 \end{bmatrix} \mathrm{v}(M^{\text{B}}). \tag{73}$$

This definition can be used to manipulate force equation (45) and dynamics equation (53) into the following affine representation with respect to $\mathrm{v}(M^{\text{B}})$

$$\begin{aligned} \boldsymbol{f}_c^{\text{B}} =& \Big[-r(\boldsymbol{a}_g^{\text{B}} + \boldsymbol{a}_{J_2}^{\text{B}}) - \left[\frac{3\mu(\boldsymbol{r}_{\text{B/I}}^{\text{B}})^{\text{s}}}{\|\boldsymbol{r}_{\text{B/I}}^{\text{B}}\|^5}\right]^{\times} r(\boldsymbol{r}_{\text{B/I}}^{\text{B}}) \\ &+ r((\dot{\boldsymbol{\omega}}_{\text{B/D}}^{\text{B}} + \boldsymbol{q}_{\text{B/D}}^{*}\dot{\boldsymbol{\omega}}_{\text{D/I}}^{\text{D}}\boldsymbol{q}_{\text{B/D}} + \boldsymbol{\omega}_{\text{D/I}}^{\text{B}} \times \boldsymbol{\omega}_{\text{B/D}}^{\text{B}})^{\text{s}}) + [(\boldsymbol{\omega}_{\text{B/D}}^{\text{B}} + \boldsymbol{\omega}_{\text{D/I}}^{\text{B}})]^{\times} r((\boldsymbol{\omega}_{\text{B/D}}^{\text{B}} + \boldsymbol{\omega}_{\text{D/I}}^{\text{B}})^{\text{s}}) \Big] \mathrm{v}(M^{\text{B}}) \\ \triangleq& \underbrace{R(\boldsymbol{r}_{\text{B/I}}^{\text{B}}, \dot{\boldsymbol{\omega}}_{\text{B/D}}^{\text{B}}, \boldsymbol{\omega}_{\text{B/D}}^{\text{B}}, \dot{\boldsymbol{\omega}}_{\text{D/I}}^{\text{D}}, \boldsymbol{\omega}_{\text{D/I}}^{\text{D}}, \boldsymbol{q}_{\text{B/D}})}_{\text{regressor matrix}} \mathrm{v}(M^{\text{B}}), \end{aligned} \tag{74}$$

where $R : \mathbb{H}_d^v \times \mathbb{H}_d^v \times \mathbb{H}_d^v \times \mathbb{H}_d^v \times \mathbb{H}_d^v \times \mathbb{H}_d^u \to \mathbb{R}^{8\times 7}$ and where we have neglected the dual disturbance force. Dropping the arguments of R for convenience we can define the error variable ε as

$$\varepsilon \triangleq R\mathrm{v}(\widehat{M^{\text{B}}}) - \boldsymbol{f}_c^{\text{B}}, \tag{75}$$

and using equation (74), the above equation can be re-interpreted as

$$\begin{aligned} \varepsilon &\triangleq R\mathrm{v}(\widehat{M^{\text{B}}}) - \boldsymbol{f}_c^{\text{B}} \\ &= R\mathrm{v}(\widehat{M^{\text{B}}}) - R\mathrm{v}(M^{\text{B}}) \\ &= R\left(\mathrm{v}(\widehat{M^{\text{B}}}) - \mathrm{v}(M^{\text{B}})\right) \\ &= R\mathrm{v}(\Delta M^{\text{B}}), \end{aligned} \tag{76}$$

effectively making ε a signal that quantifies the error in the dual inertia matrix for a given estimate $\mathrm{v}(\widehat{M^{\text{B}}})$. This quantification of the error in the inertia matrix is, in fact, the key step in concurrent learning, since it will allow us to introduce information about the dynamical state of the system at every timestep. At this point, it is also worth emphasizing that in generating the variable ε there is no need for the true inertia matrix parameters; only knowledge of the regressor matrix R, the *estimated* dual inertia, and the applied dual force are needed, as in equation (75).

Adaptive Controller

In this section we provide an adaptive pose-tracking controller that uses a new continuous formulation of the concurrent learning algorithm to provide strong assurances on the convergence of the mass and the inertia matrix of the spacecraft. The result is an extension of the controller first described in Reference 19, with the corrections incorporated in Reference 28. The proof closely mimics the proof provided therein with two modifications. The main modification is the incorporation of a new concurrent learning-based term which leads to improved performance in the estimation of the mass properties, while still providing a controller that can achieve the tracking objective. Second, a more logical sequence of steps for the use of Barbalat's Lemma is provided, compared to the approach followed in Reference 28.

The next theorem shows *almost* global asymptotic stability of the linear and angular motion relative to the desired reference can be ensured with this control law. Almost global asymptotic stability is the strongest kind of stability that can be proven for this problem for the given parametrization.

Theorem 1. *Consider the relative kinematic and dynamic equations given by equation* (40) *and equation* (45) *respectively. Let the dual control force be defined by the feedback control law*

$$\begin{aligned}\boldsymbol{f}_c^{\mathrm{B}} =& -\widehat{M^{\mathrm{B}}} \star \boldsymbol{a}_g^{\mathrm{B}} - \widehat{M^{\mathrm{B}}} \star \boldsymbol{a}_{J_2}^{\mathrm{B}} - \frac{3\mu(\boldsymbol{r}_{\mathrm{B/I}}^{\mathrm{B}})^{\mathsf{s}}}{\|\boldsymbol{r}_{\mathrm{B/I}}^{\mathrm{B}}\|^5} \times (\widehat{M^{\mathrm{B}}} \star \boldsymbol{r}_{\mathrm{B/I}}^{\mathrm{B}}) - \mathrm{vec}\big(\boldsymbol{q}_{\mathrm{B/D}}^*(\boldsymbol{q}_{\mathrm{B/D}}^{\mathsf{s}} - \mathsf{1}^{\mathsf{s}})\big) - K_d \star \boldsymbol{s}^{\mathsf{s}} \\ &+ \boldsymbol{\omega}_{\mathrm{B/I}}^{\mathrm{B}} \times (\widehat{M^{\mathrm{B}}} \star (\boldsymbol{\omega}_{\mathrm{B/I}}^{\mathrm{B}})^{\mathsf{s}}) + \widehat{M^{\mathrm{B}}} \star (\boldsymbol{q}_{\mathrm{B/D}}^* \dot{\boldsymbol{\omega}}_{\mathrm{D/I}}^{\mathrm{D}} \boldsymbol{q}_{\mathrm{B/D}})^{\mathsf{s}} + \widehat{M^{\mathrm{B}}} \star (\boldsymbol{\omega}_{\mathrm{D/I}}^{\mathrm{B}} \times \boldsymbol{\omega}_{\mathrm{B/D}}^{\mathrm{B}})^{\mathsf{s}} - \widehat{M^{\mathrm{B}}} \star (K_p \star \frac{\mathrm{d}}{\mathrm{d}t}(\boldsymbol{q}_{\mathrm{B/D}}^*(\boldsymbol{q}_{\mathrm{B/D}}^{\mathsf{s}} - \mathsf{1}^{\mathsf{s}}))), \end{aligned} \tag{77}$$

where

$$\boldsymbol{s} = \boldsymbol{\omega}_{\mathrm{B/D}}^{\mathrm{B}} + (K_p \star (\boldsymbol{q}_{\mathrm{B/D}}^*(\boldsymbol{q}_{\mathrm{B/D}}^{\mathsf{s}} - \mathsf{1}^{\mathsf{s}})))^{\mathsf{s}}, \tag{78}$$

$$K_p = \begin{bmatrix} K_r & 0_{4\times4} \\ 0_{4\times4} & K_q \end{bmatrix}, \; K_r = \begin{bmatrix} 0 & 0_{1\times3} \\ 0_{3\times1} & \bar{K}_r \end{bmatrix}, \; K_q = \begin{bmatrix} 0 & 0_{1\times3} \\ 0_{3\times1} & \bar{K}_q \end{bmatrix}, \tag{79}$$

$$K_d = \begin{bmatrix} K_v & 0_{4\times4} \\ 0_{4\times4} & K_\omega \end{bmatrix}, \; K_v = \begin{bmatrix} 0 & 0_{1\times3} \\ 0_{3\times1} & \bar{K}_v \end{bmatrix}, \; K_\omega = \begin{bmatrix} 0 & 0_{1\times3} \\ 0_{3\times1} & \bar{K}_\omega \end{bmatrix}, \tag{80}$$

and $\bar{K}_r, \bar{K}_q, \bar{K}_v, \bar{K}_\omega \in \mathbb{R}^{3\times3}$ *are positive definite matrices,* $\widehat{M^{\mathrm{B}}}$ *is an estimate of* M^{B} *updated according to*

$$\begin{aligned}\frac{\mathrm{d}}{\mathrm{d}t}\mathrm{v}(\widehat{M^{\mathrm{B}}}) =& -\alpha K_i \left(\mathsf{P}\mathrm{v}(\widehat{M^{\mathrm{B}}}) - \mathsf{Q}\right) + K_i\Big[-\mathrm{h}((\boldsymbol{s} \times \boldsymbol{\omega}_{\mathrm{B/I}}^{\mathrm{B}})^{\mathsf{s}}, (\boldsymbol{\omega}_{\mathrm{B/I}}^{\mathrm{B}})^{\mathsf{s}}) + \mathrm{h}(\boldsymbol{s}^{\mathsf{s}}, \boldsymbol{a}_g^{\mathrm{B}}) + \mathrm{h}(\boldsymbol{s}^{\mathsf{s}}, \boldsymbol{a}_{J_2}^{\mathrm{B}}) \\ &+ \mathrm{h}((\boldsymbol{s} \times \frac{3\mu(\boldsymbol{r}_{\mathrm{B/I}}^{\mathrm{B}})^{\mathsf{s}}}{\|\boldsymbol{r}_{\mathrm{B/I}}^{\mathrm{B}}\|^5})^{\mathsf{s}}, \boldsymbol{r}_{\mathrm{B/I}}^{\mathrm{B}}) - \mathrm{h}(\boldsymbol{s}^{\mathsf{s}}, (\boldsymbol{q}_{\mathrm{B/D}}^* \dot{\boldsymbol{\omega}}_{\mathrm{D/I}}^{\mathrm{D}} \boldsymbol{q}_{\mathrm{B/D}})^{\mathsf{s}} + (\boldsymbol{\omega}_{\mathrm{D/I}}^{\mathrm{B}} \times \boldsymbol{\omega}_{\mathrm{B/D}}^{\mathrm{B}})^{\mathsf{s}} - K_p \star \frac{\mathrm{d}(q_{\mathrm{B/D}}^*(q_{\mathrm{B/D}}^{\mathsf{s}} - \mathsf{1}^{\mathsf{s}}))}{\mathrm{d}t})\Big], \end{aligned} \tag{81}$$

where $\alpha > 0$*,* $K_i \in \mathbb{R}^{7\times7}$ *is a positive definite matrix, the function* $\mathrm{h} : \mathbb{H}_d^v \times \mathbb{H}_d^v \to \mathbb{R}^7$ *is defined as* $\boldsymbol{a} \circ (M^B \star \boldsymbol{b}) =$

$\mathrm{h}(\boldsymbol{a},\boldsymbol{b})^{\mathsf{T}}\mathrm{v}(M^B) = \mathrm{v}(M^B)^{\mathsf{T}}\mathrm{h}(\boldsymbol{a},\boldsymbol{b})$ *or, equivalently,* $\mathrm{h}(\boldsymbol{a},\boldsymbol{b}) = [a_6b_6,\ a_7b_6{+}a_6b_7,\ a_8b_6{+}a_6b_8,\ a_7b_7,\ a_8b_7{+}a_7b_8,\ a_8b_8,\ a_2b_2{+}a_3b_3{+}a_4b_4]^{\mathsf{T}}$*, and* $\mathsf{P} \in \mathbb{R}^{7\times 7}$ *and* $\mathsf{Q} \in \mathbb{R}^7$ *evolve as*

$$\mathsf{P}(t) = \int_{t-\tau}^{t} R^{\mathsf{T}} R \,\mathrm{d}t, \qquad \mathsf{P}(t-\tau) = 0_{7\times 7} \text{ and } \tau > 0, \tag{82}$$

and

$$\mathsf{Q}(t) = \int_{t-\tau}^{t} R^{\mathsf{T}} \boldsymbol{f}_c^{\mathrm{B}} \,\mathrm{d}t, \qquad \mathsf{Q}(t-\tau) = 0_{7\times 1} \text{ and } \tau > 0, \tag{83}$$

where R *and* $\boldsymbol{f}_c^{\mathrm{B}}$ *are defined as in equation* (74)*. Assume that* $\boldsymbol{q}_{\mathrm{D/I}}, \boldsymbol{\omega}_{\mathrm{D/I}}^{\mathrm{D}}, \dot{\boldsymbol{\omega}}_{\mathrm{D/I}}^{\mathrm{D}} \in \mathcal{L}_\infty$*. Then, for all initial conditions,* $\lim_{t\to\infty} \boldsymbol{q}_{\mathrm{B/D}} = \pm\mathtt{1}$ *(i.e.,* $\lim_{t\to\infty} q_{\mathrm{B/D}} = \pm\mathtt{1}$ *and* $\lim_{t\to\infty} r_{\mathrm{B/D}}^{\mathrm{B}} = \mathtt{0}$*), and* $\lim_{t\to\infty} \boldsymbol{\omega}_{\mathrm{B/D}}^{\mathrm{B}} = \mathtt{0}$ *(i.e.,* $\lim_{t\to\infty} \omega_{\mathrm{B/D}}^{\mathrm{B}} = \mathtt{0}$ *and* $\lim_{t\to\infty} v_{\mathrm{B/D}}^{\mathrm{B}} = \mathtt{0}$*).*

If, in addition,

$$\operatorname{rank} \mathsf{P}(t) = 7, \tag{84}$$

then $\lim_{t\to\infty} \mathrm{v}(\widehat{M^{\mathrm{B}}}) = \mathrm{v}(M^{\mathrm{B}})$.

Proof. Note that $\boldsymbol{q}_{\mathrm{B/D}} = \pm\mathtt{1}$, $\boldsymbol{s} = \mathtt{0}$, and $\mathrm{v}(\varDelta M^{\mathrm{B}}) = 0_{7\times 1}$ are the equilibrium conditions of the closed-loop system with dynamics given by equation (45), kinematics described by equation (40), feedback control law given by equation (77), and a dual inertia matrix update as in equation (81), with P and $\mathsf{Q}(t)$ evolving as described by equations (82) and (83). Consider now the following candidate Lyapunov function for the equilibrium point $(\boldsymbol{q}_{\mathrm{B/D}}, \boldsymbol{s}, \mathrm{v}(\varDelta M^{\mathrm{B}})) = (+\mathtt{1}, \mathtt{0}, 0_{7\times 1})$:

$$V(\boldsymbol{q}_{\mathrm{B/D}}, \boldsymbol{s}, \mathrm{v}(\varDelta M^{\mathrm{B}})) = (\boldsymbol{q}_{\mathrm{B/D}} - \mathtt{1}) \circ (\boldsymbol{q}_{\mathrm{B/D}} - \mathtt{1}) + \tfrac{1}{2}\boldsymbol{s}^{\mathsf{s}} \circ (M^{\mathrm{B}} \star \boldsymbol{s}^{\mathsf{s}}) + \tfrac{1}{2}\mathrm{v}(\varDelta M^{\mathrm{B}})^{\mathsf{T}} K_i^{-1} \mathrm{v}(\varDelta M^{\mathrm{B}}). \tag{85}$$

Note that V is a valid candidate Lyapunov function since

$$V(\boldsymbol{q}_{\mathrm{B/D}} = \mathtt{1}, \boldsymbol{s} = \mathtt{0}, \mathrm{v}(\varDelta M^{\mathrm{B}}) = 0_{7\times 1}) = 0,$$

and

$$V(\boldsymbol{q}_{\mathrm{B/D}}, \boldsymbol{s}, \mathrm{v}(\varDelta M^{\mathrm{B}})) > 0, \quad \forall (\boldsymbol{q}_{\mathrm{B/D}}, \boldsymbol{s}, \mathrm{v}(\varDelta M^{\mathrm{B}})) \in \mathbb{H}_d^u \times \mathbb{H}_d^v \times \mathbb{R}^7 \backslash \{\mathtt{1}, \mathtt{0}, 0_{7\times 1}\}.$$

The time derivative of V is equal to

$$\dot{V} = 2(\boldsymbol{q}_{\mathrm{B/D}} - \mathtt{1}) \circ \dot{\boldsymbol{q}}_{\mathrm{B/D}} + \boldsymbol{s}^{\mathsf{s}} \circ (M^{\mathrm{B}} \star \dot{\boldsymbol{s}}^{\mathsf{s}}) + \mathrm{v}(\varDelta M^{\mathrm{B}})^{\mathsf{T}} K_i^{-1} \frac{\mathrm{d}\mathrm{v}(\varDelta M^{\mathrm{B}})}{\mathrm{d}t}.$$

From equation (40) and equation (78) we can write $\dot{\boldsymbol{q}}_{\mathrm{B/D}} = \frac{1}{2}\boldsymbol{q}_{\mathrm{B/D}}\boldsymbol{s} - \frac{1}{2}\boldsymbol{q}_{\mathrm{B/D}}(K_p \star (\boldsymbol{q}_{\mathrm{B/D}}^{*}(\boldsymbol{q}_{\mathrm{B/D}}^{\mathsf{s}} - \mathtt{1}^{\mathsf{s}})))^{\mathsf{s}}$, which can then be plugged into $\dot{V}$, together with the time derivative of equation (78), to yield

$$\dot{V}=(\boldsymbol{q}_{\text{B/D}}-\mathsf{1})\circ(\boldsymbol{q}_{\text{B/D}}\boldsymbol{s}-\boldsymbol{q}_{\text{B/D}}(K_p\star(\boldsymbol{q}^*_{\text{B/D}}(\boldsymbol{q}^{\mathsf{s}}_{\text{B/D}}-\mathsf{1}^{\mathsf{s}})))^{\mathsf{s}})+\mathrm{v}(\varDelta M^{\text{B}})^{\mathsf{T}}K_i^{-1}\frac{\mathrm{d}}{\mathrm{d}t}\mathrm{v}(\varDelta M^{\text{B}})$$
$$+\boldsymbol{s}^{\mathsf{s}}\circ(M^{\text{B}}\star(\dot{\boldsymbol{\omega}}^{\text{B}}_{\text{B/D}})^{\mathsf{s}})+\boldsymbol{s}^{\mathsf{s}}\circ(M^{\text{B}}\star(K_p\star\frac{\mathrm{d}(q^*_{\text{B/D}}(q^{\mathsf{s}}_{\text{B/D}}-\mathsf{1}^{\mathsf{s}}))}{\mathrm{d}t})).$$

Applying equation (32) to the first term, evaluating the dynamics from equation (45) with the force defined by equation (53), neglecting the disturbance dual force, and using the identity $\boldsymbol{\omega}^{\text{B}}_{\text{B/D}}+\boldsymbol{\omega}^{\text{B}}_{\text{D/I}}=\boldsymbol{\omega}^{\text{B}}_{\text{B/I}}$ yields

$$\dot{V}=-(K_p\star(\boldsymbol{q}^*_{\text{B/D}}(\boldsymbol{q}^{\mathsf{s}}_{\text{B/D}}-\mathsf{1}^{\mathsf{s}})))\circ(\boldsymbol{q}^*_{\text{B/D}}(\boldsymbol{q}^{\mathsf{s}}_{\text{B/D}}-\mathsf{1}^{\mathsf{s}}))+\boldsymbol{s}^{\mathsf{s}}\circ(M^{\text{B}}\star\boldsymbol{a}^{\text{B}}_g+\frac{3\mu(\boldsymbol{r}^{\text{B}}_{\text{B/I}})^{\mathsf{s}}}{\|\boldsymbol{r}^{\text{B}}_{\text{B/I}}\|^5}\times(M^{\text{B}}\star\boldsymbol{r}^{\text{B}}_{\text{B/I}})+M^{\text{B}}\star\boldsymbol{a}^{\text{B}}_{J_2}+\boldsymbol{f}^{\text{B}}_c$$
$$-\boldsymbol{\omega}^{\text{B}}_{\text{B/I}}\times\big(M^{\text{B}}\star(\boldsymbol{\omega}^{\text{B}}_{\text{B/I}})^{\mathsf{s}}\big)-M^{\text{B}}\star(\boldsymbol{q}^*_{\text{B/D}}\dot{\boldsymbol{\omega}}^{\text{D}}_{\text{D/I}}\boldsymbol{q}_{\text{B/D}})^{\mathsf{s}}-M^{\text{B}}\star(\boldsymbol{\omega}^{\text{B}}_{\text{D/I}}\times\boldsymbol{\omega}^{\text{B}}_{\text{B/D}})^{\mathsf{s}})+\boldsymbol{s}^{\mathsf{s}}\circ(M^{\text{B}}\star(K_p\star\frac{\mathrm{d}(q^*_{\text{B/D}}(q^{\mathsf{s}}_{\text{B/D}}-\mathsf{1}^{\mathsf{s}}))}{\mathrm{d}t}))$$
$$+\mathrm{v}(\varDelta M^{\text{B}})^{\mathsf{T}}K_i^{-1}\frac{\mathrm{d}}{\mathrm{d}t}\mathrm{v}(\varDelta M^{\text{B}})+\boldsymbol{s}^{\mathsf{s}}\circ(\boldsymbol{q}^*_{\text{B/D}}(\boldsymbol{q}^{\mathsf{s}}_{\text{B/D}}-\mathsf{1}^{\mathsf{s}})).$$

Introducing the feedback control law for $\boldsymbol{f}^{\text{B}}_c$ given by equation (77) and using equations (31) and (33) yields

$$\dot{V}=-(\boldsymbol{q}^*_{\text{B/D}}(\boldsymbol{q}^{\mathsf{s}}_{\text{B/D}}-\mathsf{1}^{\mathsf{s}}))\circ(K_p\star(\boldsymbol{q}^*_{\text{B/D}}(\boldsymbol{q}^{\mathsf{s}}_{\text{B/D}}-\mathsf{1}^{\mathsf{s}})))+\boldsymbol{s}^{\mathsf{s}}\circ(-\varDelta M^{\text{B}}\star\boldsymbol{a}^{\text{B}}_g-\frac{3\mu(\boldsymbol{r}^{\text{B}}_{\text{B/I}})^{\mathsf{s}}}{\|\boldsymbol{r}^{\text{B}}_{\text{B/I}}\|^5}\times(\varDelta M^{\text{B}}\star\boldsymbol{r}^{\text{B}}_{\text{B/I}})$$
$$-\varDelta M^{\text{B}}\star\boldsymbol{a}^{\text{B}}_{J_2}+\boldsymbol{\omega}^{\text{B}}_{\text{B/I}}\times\big(\varDelta M^{\text{B}}\star(\boldsymbol{\omega}^{\text{B}}_{\text{B/I}})^{\mathsf{s}}\big)+\varDelta M^{\text{B}}\star(\boldsymbol{q}^*_{\text{B/D}}\dot{\boldsymbol{\omega}}^{\text{D}}_{\text{D/I}}\boldsymbol{q}_{\text{B/D}})^{\mathsf{s}}+\varDelta M^{\text{B}}\star(\boldsymbol{\omega}^{\text{B}}_{\text{D/I}}\times\boldsymbol{\omega}^{\text{B}}_{\text{B/D}})^{\mathsf{s}}$$
$$-\varDelta M^{\text{B}}\star(K_p\star\frac{\mathrm{d}(q^*_{\text{B/D}}(q^{\mathsf{s}}_{\text{B/D}}-\mathsf{1}^{\mathsf{s}}))}{\mathrm{d}t}))-\boldsymbol{s}^{\mathsf{s}}\circ(K_d\star\boldsymbol{s}^{\mathsf{s}})+\mathrm{v}(\varDelta M^{\text{B}})^{\mathsf{T}}K_i^{-1}\frac{\mathrm{d}}{\mathrm{d}t}\mathrm{v}(\varDelta M^{\text{B}})$$

or

$$\dot{V}=-(\boldsymbol{q}^*_{\text{B/D}}(\boldsymbol{q}^{\mathsf{s}}_{\text{B/D}}-\mathsf{1}^{\mathsf{s}}))\circ(K_p\star(\boldsymbol{q}^*_{\text{B/D}}(\boldsymbol{q}^{\mathsf{s}}_{\text{B/D}}-\mathsf{1}^{\mathsf{s}})))-\boldsymbol{s}^{\mathsf{s}}\circ(\varDelta M^{\text{B}}\star\boldsymbol{a}^{\text{B}}_g)-\left(\boldsymbol{s}\times\frac{3\mu(\boldsymbol{r}^{\text{B}}_{\text{B/I}})^{\mathsf{s}}}{\|\boldsymbol{r}^{\text{B}}_{\text{B/I}}\|^5}\right)^{\mathsf{s}}\circ(\varDelta M^{\text{B}}\star\boldsymbol{r}^{\text{B}}_{\text{B/I}})$$
$$-\boldsymbol{s}^{\mathsf{s}}\circ(\varDelta M^{\text{B}}\star\boldsymbol{a}^{\text{B}}_{J_2})+\boldsymbol{s}^{\mathsf{s}}\circ(\varDelta M^{\text{B}}\star(\boldsymbol{q}^*_{\text{B/D}}\dot{\boldsymbol{\omega}}^{\text{D}}_{\text{D/I}}\boldsymbol{q}_{\text{B/D}})^{\mathsf{s}}+\varDelta M^{\text{B}}\star(\boldsymbol{\omega}^{\text{B}}_{\text{D/I}}\times\boldsymbol{\omega}^{\text{B}}_{\text{B/D}})^{\mathsf{s}}-\varDelta M^{\text{B}}\star(K_p\star\frac{\mathrm{d}(q^*_{\text{B/D}}(q^{\mathsf{s}}_{\text{B/D}}-\mathsf{1}^{\mathsf{s}}))}{\mathrm{d}t}))$$
$$+(\boldsymbol{s}\times\boldsymbol{\omega}^{\text{B}}_{\text{B/I}})^{\mathsf{s}}\circ(\varDelta M^{\text{B}}\star(\boldsymbol{\omega}^{\text{B}}_{\text{B/I}})^{\mathsf{s}})-\boldsymbol{s}^{\mathsf{s}}\circ(K_d\star\boldsymbol{s}^{\mathsf{s}})+\mathrm{v}(\varDelta M^{\text{B}})^{\mathsf{T}}K_i^{-1}\frac{\mathrm{d}}{\mathrm{d}t}\mathrm{v}(\varDelta M^{\text{B}}).$$

Also notice from equation (82) that

$$\mathsf{P}(t)=\int_{t-\tau}^{t}R^{\mathsf{T}}R\,\mathrm{d}t\geq 0. \tag{86}$$

Using equations (82) and (83), we have

$$\mathsf{P}(t)\mathrm{v}(\widehat{M^{\text{B}}})-\mathsf{Q}(t)=\int_{t-\tau}^{t}R^{\mathsf{T}}R\,\mathrm{d}t\mathrm{v}(\widehat{M^{\text{B}}})-\int_{t-\tau}^{t}R^{\mathsf{T}}\boldsymbol{f}^{\text{B}}_c\,\mathrm{d}t. \tag{87}$$

Using equation (74), we then obtain

$$
\begin{aligned}
\mathsf{P}(t)\mathrm{v}(\widehat{M^{\mathrm{B}}}) - \mathsf{Q}(t) &= \int_{t-\tau}^{t} R^{\mathsf{T}} R \,\mathrm{d}t\; \mathrm{v}(\widehat{M^{\mathrm{B}}}) - \int_{t-\tau}^{t} R^{\mathsf{T}} R \mathrm{v}(M^{\mathrm{B}})\,\mathrm{d}t \\
&= \int_{t-\tau}^{t} R^{\mathsf{T}} R \,\mathrm{d}t\; \mathrm{v}(\widehat{M^{\mathrm{B}}}) - \int_{t-\tau}^{t} R^{\mathsf{T}} R \,\mathrm{d}t\; \mathrm{v}(M^{\mathrm{B}}) \\
&= \int_{t-\tau}^{t} R^{\mathsf{T}} R \,\mathrm{d}t\; \left(\mathrm{v}(\widehat{M^{\mathrm{B}}}) - \mathrm{v}(M^{\mathrm{B}})\right) \\
&= \int_{t-\tau}^{t} R^{\mathsf{T}} R \,\mathrm{d}t\; \mathrm{v}(\varDelta M^{\mathrm{B}}) \\
&= \mathsf{P}(t)\mathrm{v}(\varDelta M^{\mathrm{B}}),
\end{aligned}
\tag{88}
$$

where for the second equality we have used the assumption that the true inertia matrix is constant. Assuming again constant M^{B}, $\frac{\mathrm{d}}{\mathrm{d}t}\mathrm{v}(\varDelta M^{\mathrm{B}}) = \frac{\mathrm{d}}{\mathrm{d}t}\mathrm{v}(\widehat{M^{\mathrm{B}}})$, so evaluating equation (81), and using the relationship in equation (88), it follows that

$$
\begin{aligned}
\dot{V} = &-(\boldsymbol{q}^*_{\mathrm{B/D}}(\boldsymbol{q}^{\mathsf{s}}_{\mathrm{B/D}} - \mathtt{1}^{\mathsf{s}})) \circ (K_p \star (\boldsymbol{q}^*_{\mathrm{B/D}}(\boldsymbol{q}^{\mathsf{s}}_{\mathrm{B/D}} - \mathtt{1}^{\mathsf{s}}))) - \boldsymbol{s}^{\mathsf{s}} \circ (K_d \star \boldsymbol{s}^{\mathsf{s}}) \\
&-\alpha \mathrm{v}(\varDelta M^{\mathrm{B}})^{\mathsf{T}} \mathsf{P}(t) \mathrm{v}(\varDelta M^{\mathrm{B}}) \le 0,
\end{aligned}
\tag{89}
$$

for all $(\boldsymbol{q}_{\mathrm{B/D}}, \boldsymbol{s}, \mathrm{v}(\varDelta M^{\mathrm{B}})) \in \mathbb{H}^u_d \times \mathbb{H}^v_d \times \mathbb{R}^7 \backslash \{\mathtt{1}, \mathtt{0}, 0_{7\times 1}\}$. Hence, the equilibrium point $(\boldsymbol{q}_{\mathrm{B/D}}, \boldsymbol{s}, \mathrm{v}(\varDelta M^{\mathrm{B}})) = (+\mathtt{1}, \mathtt{0}, 0_{7\times 1})$ is uniformly stable and the solutions are uniformly bounded, i.e., $\boldsymbol{q}_{\mathrm{B/D}}, \boldsymbol{s}, \mathrm{v}(\varDelta M^{\mathrm{B}}), \in \mathcal{L}_\infty$. Moreover, from equations (72) and (78) it follows that $\boldsymbol{\omega}^{\mathrm{B}}_{\mathrm{B/D}}, \mathrm{v}(\widehat{M^{\mathrm{B}}}) \in \mathcal{L}_\infty$. Since $V \ge 0$ and $\dot{V} \le 0$, $\lim_{t\to\infty} V(t)$ exists and is finite. Hence, $\lim_{t\to\infty} \int_0^t \dot{V}(\tau)\,\mathrm{d}\tau = \lim_{t\to\infty} V(t) - V(0)$ also exists and is finite. Since $\boldsymbol{q}_{\mathrm{B/D}}$, $\boldsymbol{s}$, $\mathrm{v}(\varDelta M^{\mathrm{B}})$, $\boldsymbol{\omega}^{\mathrm{B}}_{\mathrm{B/D}}$, $\mathrm{v}(\widehat{M^{\mathrm{B}}})$, $\dot{\boldsymbol{\omega}}^{\mathrm{D}}_{\mathrm{D/I}}$, $\boldsymbol{\omega}^{\mathrm{B}}_{\mathrm{D/I}}$, $\boldsymbol{q}_{\mathrm{D/I}} \in \mathcal{L}_\infty$, then from equations (40), (45) and (77) in combination with Lemma 53 in Reference 28, it follows that $r^{\mathrm{B}}_{\mathrm{B/D}}, \dot{\boldsymbol{q}}_{\mathrm{B/D}}, \boldsymbol{f}^{\mathrm{B}}, \dot{\boldsymbol{\omega}}^{\mathrm{B}}_{\mathrm{B/D}}, \dot{\boldsymbol{s}} \in \mathcal{L}_\infty$, and hence $\ddot{V}$ is bounded. Then, by Barbalat's lemma, the system trajectories approach the set for which $\dot{V} = 0$. Since $K_p = \mathrm{diag}(0, \bar{K}_r, 0, \bar{K}_q)$, this implies that $\mathrm{vec}\big(\boldsymbol{q}^*_{\mathrm{B/D}}(\boldsymbol{q}^{\mathsf{s}}_{\mathrm{B/D}} - \mathtt{1}^{\mathsf{s}})\big) \to \mathtt{0}$, $\boldsymbol{s} \to \mathtt{0}$, and $\mathsf{P}^{1/2}\mathrm{v}(\varDelta M^{\mathrm{B}}) \to 0_{7\times 1}$ as $t \to \infty$. In Reference 28 it is proven that $\mathrm{vec}\big(\boldsymbol{q}^*_{\mathrm{B/D}}(\boldsymbol{q}^{\mathsf{s}}_{\mathrm{B/D}} - \mathtt{1}^{\mathsf{s}})\big) \to \mathtt{0}$ as $t \to \infty$ implies $\boldsymbol{q}_{\mathrm{B/D}} \to \pm\mathtt{1}$ as $t \to \infty$. Furthermore, calculating the limit as $t \to \infty$ of both sides of equation (78) yields $\boldsymbol{\omega}^{\mathrm{B}}_{\mathrm{B/D}} \to \mathtt{0}$, which concludes the first part of the proof.

If, in addition, $\mathsf{P}(t)$ satisfies $\mathrm{rank}\,\mathsf{P}(t) = 7$, or equivalently $\mathsf{P}(t) > 0$, then $\dot{V} < 0$, which implies that $\mathrm{vec}\big(\boldsymbol{q}^*_{\mathrm{B/D}}(\boldsymbol{q}^{\mathsf{s}}_{\mathrm{B/D}} - \mathtt{1}^{\mathsf{s}})\big) \to \mathtt{0}$, $\boldsymbol{s} \to \mathtt{0}$, and $\mathrm{v}(\varDelta M^{\mathrm{B}}) \to 0_{7\times 1}$ as $t \to \infty$. Through analogous arguments, we conclude that $\boldsymbol{q}_{\mathrm{B/D}} \to \pm\mathtt{1}$, and $\boldsymbol{\omega}^{\mathrm{B}}_{\mathrm{B/D}} \to \mathtt{0}$. Therefore, by the definition of ΔM^{B}, we conclude that $\mathrm{v}(\widehat{M^{\mathrm{B}}}) \to \mathrm{v}(M^{\mathrm{B}})$ as $t \to \infty$. □

Remark 1. For the case in which $\mathrm{rank}\,\mathsf{P}(t) = 7$, or equivalently $\mathsf{P}(t) > 0$ for some $t > T$, it is possible to directly prove that $\mathrm{v}(\varDelta M^{\mathrm{B}}) \to 0_{7\times 1}$ because the term

$$
-\alpha \mathrm{v}(\varDelta M^{\mathrm{B}})^{\mathsf{T}} \mathsf{P}(t) \mathrm{v}(\varDelta M^{\mathrm{B}})
$$

appears in the derivative of the Lyapunov function, which is the main contribution of the concurrent learning framework. Note that to do this, the manipulation of the dynamical system into the form of equation (76) was key.

Remark 2. Theorem 1 ensures *almost* global asymptotic stability since we can only ensure $\boldsymbol{q}_{\mathrm{B/D}} \to \pm\mathtt{1}$ as $t \to \infty$, and not simply $\boldsymbol{q}_{\mathrm{B/D}} \to \mathtt{1}$ as $t \to \infty$. The existence of an equilibrium point of the closed loop system at the unstable pole $\boldsymbol{q}_{\mathrm{B/D}} \to -\mathtt{1}$ will give rise to the *unwinding phenomenon*. For an approach to deal with this phenomenon, the reader is referred to Reference 39, which proposes a robust, hybrid controller of similar form to that of References 19, 20, 31.

Remark 3. The matrix $\mathsf{P}(t)$ is positive semi-definite (except at time $t - \tau$, when it is initialized) by construction. By the same token, the integration in equation (86) is unbounded. Appropriate monitoring of the rank condition must be enforced so that once the rank condition in equation (84) is satisfied, α can eventually be set to $\alpha = 0$ to avoid numerical problems in the control law. For this reason, a discrete implementation of concurrent learning is a reasonable substitute. Discretizing the collection of data allows bounding the growth of the largest singular values of $\mathsf{P}(t)$.

Remark 4. As pointed out in Reference 43, in real systems linear and angular velocity measurements, are inevitably corrupted by noise. This limitation is not considered in this work and will be the subject of future research. In fact, the concurrent learning framework has already been successfully tested experimentally.[44] In practice, the derivatives of certain states might not be readily accessible through the measurements. This is the case, for example, with $\dot{\boldsymbol{\omega}}^{\mathrm{B}}_{\mathrm{B/D}}$. An optimal fixed-point smoother can be used to estimate these variables.[42,44] A Butterworth filter applied to $\boldsymbol{\omega}^{\mathrm{B}}_{\mathrm{B/D}}$ has also been observed to capture the evolution of $\dot{\boldsymbol{\omega}}^{\mathrm{B}}_{\mathrm{B/D}}$ accurately when differentiated in the s-domain. Appropriate corrections for the lag introduced by the estimators or filters have to be made in this case.

Concurrent Learning as a Contributing Factor to Meet Persistency of Excitation Conditions

In this section we provide an approach to incorporate the concurrent learning rank condition given in equation (84) into the analysis of convergence of the estimation parameters in the context of persistency of excitation (PE).

Consider the system with kinematics dictated by equation (40) and relative dynamics given by equation (45). If we evaluate the control law proposed in Theorem 1 we obtain the closed-loop system described by the following set of equations:

$$\dot{\boldsymbol{q}}_{\mathrm{B/D}} = \tfrac{1}{2}\boldsymbol{q}_{\mathrm{B/D}}\boldsymbol{\omega}^{\mathrm{B}}_{\mathrm{B/D}} \tag{90}$$

$$\begin{aligned} M^{\mathrm{B}}\star(\dot{\boldsymbol{\omega}}^{\mathrm{B}}_{\mathrm{B/D}})^{\mathsf{s}} = &-\Delta M^{\mathrm{B}}\star\boldsymbol{a}^{\mathrm{B}}_{g} - \frac{3\mu(\boldsymbol{r}^{\mathrm{B}}_{\mathrm{B/I}})^{\mathsf{s}}}{\|\boldsymbol{r}^{\mathrm{B}}_{\mathrm{B/I}}\|^{5}}\times(\Delta M^{\mathrm{B}}\star\boldsymbol{r}^{\mathrm{B}}_{\mathrm{B/I}}) - \Delta M^{\mathrm{B}}\star\boldsymbol{a}^{\mathrm{B}}_{J_2} - \mathrm{vec}\big(\boldsymbol{q}^{*}_{\mathrm{B/D}}(\boldsymbol{q}^{\mathsf{s}}_{\mathrm{B/D}} - \mathtt{1}^{\mathsf{s}})\big) - K_d\star\boldsymbol{s}^{\mathsf{s}} \\ &+\boldsymbol{\omega}^{\mathrm{B}}_{\mathrm{B/I}}\times(\Delta M^{\mathrm{B}}\star(\boldsymbol{\omega}^{\mathrm{B}}_{\mathrm{B/I}})^{\mathsf{s}}) + \Delta M^{\mathrm{B}}\star(\boldsymbol{q}^{*}_{\mathrm{B/D}}\dot{\boldsymbol{\omega}}^{\mathrm{D}}_{\mathrm{D/I}}\boldsymbol{q}_{\mathrm{B/D}})^{\mathsf{s}} + \Delta M^{\mathrm{B}}\star(\boldsymbol{\omega}^{\mathrm{B}}_{\mathrm{D/I}}\times\boldsymbol{\omega}^{\mathrm{B}}_{\mathrm{B/D}})^{\mathsf{s}} - \widehat{M^{\mathrm{B}}}\star\Big(K_p\star\frac{\mathrm{d}}{\mathrm{d}t}\big(\boldsymbol{q}^{*}_{\mathrm{B/D}}(\boldsymbol{q}^{\mathsf{s}}_{\mathrm{B/D}} - \mathtt{1}^{\mathsf{s}})\big)\Big)^{\mathsf{s}} \end{aligned} \tag{91}$$

with $\widehat{M^{\text{B}}}$ updated as

$$\frac{\mathrm{d}}{\mathrm{d}t}\mathrm{v}(\widehat{M^{\text{B}}}) = -\alpha K_i \mathsf{P}\mathrm{v}(\Delta M^{\text{B}}) + K_i\Big[-\mathrm{h}((\boldsymbol{s}\times\boldsymbol{\omega}^{\text{B}}_{\text{B/I}})^{\mathsf{s}}, (\boldsymbol{\omega}^{\text{B}}_{\text{B/I}})^{\mathsf{s}}) + \mathrm{h}(\boldsymbol{s}^{\mathsf{s}}, \boldsymbol{a}^{\text{B}}_{g}) + \mathrm{h}(\boldsymbol{s}^{\mathsf{s}}, \boldsymbol{a}^{\text{B}}_{J_2}) + \mathrm{h}((\boldsymbol{s}\times\frac{3\mu(\boldsymbol{r}^{\text{B}}_{\text{B/I}})^{\mathsf{s}}}{\|\boldsymbol{r}^{\text{B}}_{\text{B/I}}\|^5})^{\mathsf{s}}, \boldsymbol{r}^{\text{B}}_{\text{B/I}}) - \mathrm{h}(\boldsymbol{s}^{\mathsf{s}}, (\boldsymbol{q}^*_{\text{B/D}}\dot{\boldsymbol{\omega}}^{\text{D}}_{\text{D/I}}\boldsymbol{q}_{\text{B/D}})^{\mathsf{s}} + (\boldsymbol{\omega}^{\text{B}}_{\text{D/I}}\times\boldsymbol{\omega}^{\text{B}}_{\text{B/D}})^{\mathsf{s}} - K_p\star\frac{\mathrm{d}(q^*_{\text{B/D}}(q^{\mathsf{s}}_{\text{B/D}} - \mathtt{1}^{\mathsf{s}}))}{\mathrm{d}t})\Big], \quad (92)$$

where we have dropped the dependence of $\mathsf{P}(t)$ on time for the sake of exposition.

In the Lyapunov analysis provided in the proof of Theorem 1, we concluded that $\boldsymbol{\omega}^{\text{B}}_{\text{B/D}} \to \mathtt{0}$, $\boldsymbol{s} \to \mathtt{0}$, and $\boldsymbol{q}_{\text{B/D}} \to \mathtt{1}$ as $t \to \infty$. We can prove that $\dot{\boldsymbol{\omega}}^{\text{B}}_{\text{B/D}} \to \mathtt{0}$ as follows. We know that

$$\lim_{t\to\infty}\int_0^t \dot{\boldsymbol{\omega}}^{\text{B}}_{\text{B/D}}\,\mathrm{d}t = \lim_{t\to\infty}\boldsymbol{\omega}^{\text{B}}_{\text{B/D}}(t) - \boldsymbol{\omega}^{\text{B}}_{\text{B/D}}(0) = -\boldsymbol{\omega}^{\text{B}}_{\text{B/D}}(0)$$

exists and is finite. We also know that $\boldsymbol{q}_{\text{D/I}}$, $\boldsymbol{\omega}^{\text{D}}_{\text{D/I}}$, $\dot{\boldsymbol{\omega}}^{\text{D}}_{\text{D/I}}$, $\ddot{\boldsymbol{\omega}}^{\text{D}}_{\text{D/I}}$, $\dot{\boldsymbol{q}}_{\text{B/D}}$, $\ddot{\boldsymbol{q}}_{\text{B/D}}$, $\dot{\boldsymbol{\omega}}^{\text{B}}_{\text{B/D}}$, $\mathrm{dv}(\widehat{M^{\text{B}}})/\mathrm{d}t \in \mathcal{L}_\infty$, from which it follows that $\ddot{\boldsymbol{\omega}}^{\text{B}}_{\text{B/D}} \in \mathcal{L}_\infty$ by differentiating the dynamics equation (45). By Barbalat's Lemma, $\lim_{t\to\infty}\dot{\boldsymbol{\omega}}^{\text{B}}_{\text{B/D}} = \mathtt{0}$. Therefore, taking the limit as $t \to \infty$ of equation (91), we obtain

$$\begin{aligned}\mathtt{0} &= \lim_{t\to\infty} -\Delta M^{\text{B}}\star\boldsymbol{a}^{\text{D}}_{g} - \frac{3\mu(\boldsymbol{r}^{\text{D}}_{\text{D/I}})^{\mathsf{s}}}{\|\boldsymbol{r}^{\text{D}}_{\text{D/I}}\|^5}\times(\Delta M^{\text{B}}\star\boldsymbol{r}^{\text{D}}_{\text{D/I}}) - \Delta M^{\text{B}}\star\boldsymbol{a}^{\text{D}}_{J_2} + \boldsymbol{\omega}^{\text{D}}_{\text{D/I}}\times(\Delta M^{\text{B}}\star(\boldsymbol{\omega}^{\text{D}}_{\text{D/I}})^{\mathsf{s}}) + \Delta M^{\text{B}}\star(\dot{\boldsymbol{\omega}}^{\text{D}}_{\text{D/I}})^{\mathsf{s}} \\ &\triangleq \lim_{t\to\infty}\mathrm{W}(t)\mathrm{v}(\Delta M^{\text{B}}),\end{aligned} \quad (93)$$

where $\mathrm{W} : [0,\infty) \to \mathbb{R}^{8\times 7}$ is defined explicitly by Filipe[28] .

From Barbalat's Lemma in Theorem 1, we also concluded that $\boldsymbol{s} \to \mathtt{0}$ and $\mathsf{P}^{1/2}(t)\mathrm{v}(\Delta M^{\text{B}}) \to 0$ as $t \to \infty$. Therefore, equation (92) becomes identically zero at $t \to \infty$. If we preserve the term associated to concurrent learning, we obtain

$$0 = \lim_{t\to\infty}\alpha K_i\mathsf{P}(t)\mathrm{v}(\Delta M^{\text{B}}) = \lim_{t\to\infty}\alpha\mathsf{P}(t)\mathrm{v}(\Delta M^{\text{B}}). \quad (94)$$

Equations (93) and (94) can be combined as

$$\begin{bmatrix}\mathtt{0}\\ 0\end{bmatrix} = \lim_{t\to\infty}\begin{bmatrix}\mathrm{W}(t)\\ \alpha\mathsf{P}(t)\end{bmatrix}\mathrm{v}(\Delta M^{\text{B}}) \quad (95)$$

Therefore, the condition for persistency of excitation including participation of a concurrent learning term can be cast as

$$\int_{t_1}^{t_1+T_2}\begin{bmatrix}\mathrm{W}(t)\\ \alpha\mathsf{P}(t)\end{bmatrix}^{\mathsf{T}}\begin{bmatrix}\mathrm{W}(t)\\ \alpha\mathsf{P}(t)\end{bmatrix}\,\mathrm{d}t > 0, \quad (96)$$

for all $t > T_1$ for some $T_1 > 0$ and $T_2 > 0$, which can be equivalently rewritten as

$$\int_{t_1}^{t_1+T_2} \mathrm{W}(t)^\intercal \mathrm{W}(t) + \alpha^2 \mathsf{P}^\intercal(t)\mathsf{P}(t)\,\mathrm{d}t > 0. \tag{97}$$

Several remarks are in order.

Remark 5. It is clear from the form of equation (97) that the rank condition $\operatorname{rank}\mathsf{P}(t) = 7$ in equation (84) immediately satisfies the persistency of excitation requirement.

Remark 6. For the estimation task, since $\mathsf{P}(t) \geq 0$, the proposed adaptive controllers will perform at least the same, but likely better, than the baseline controller without concurrent learning. Since the rank of the matrix $\mathsf{P}(t)$ depends on the dynamical information of the system, a clear advantage of the control scheme arises for the case of stabilization tasks, especially if these are performed in deep space. In such a case, $\boldsymbol{\omega}^{\mathrm{D}}_{\mathrm{D/I}} = \mathsf{0}$ and the small gravitational effects will yield an ill-conditioned $\mathrm{W}(t)$ matrix. The numerical example in the next section demonstrates this point.

Remark 7. For the case $\alpha = 0$, which represents no contribution from the concurrent learning algorithm to the estimation of the mass parameters in equation (81), the requirement for parameter convergence given in equation (97) collapses to the better known requirement of persistency of excitation

$$\int_{t_1}^{t_1+T_2} \mathrm{W}(t)^\intercal \mathrm{W}(t)\,\mathrm{d}t > 0, \tag{98}$$

for all $t > T_1$ for some $T_1 > 0$ and $T_2 > 0$.

NUMERICAL SIMULATIONS

The controller proposed in Theorem 1 was simulated using Simulink's ODE45 solver, and its performance was compared to that of the nominal controller proposed in Reference 20. First, a scenario in Earth orbit is investigated and later on a more challenging scenario in deep space is demonstrated. The latter case is more challenging since persistency of excitation is more difficult to satisfy owing to the absence of the additional gravitational terms. It is shown that in both cases the CL approach ensures parameter convergence even in the absence of persistency of excitation.

In the first scenario, an orbiting spacecraft will perform an orbital circumnavigation of a target satellite, an example detailed in Reference 21. The target satellite orbits in a highly eccentric Molniya orbit with altitude 813.2 km, eccentricity of 0.7, an inclination of 63.4^o, argument of periapsis of 270^o, longitude of the ascending node of 329.6^o, and true anomaly of 270^o. The orbit is subject to J_2 perturbations. The target's reference frame T is such that K_{T} is aligned with the orbital angular momentum vector, I_{T} is aligned with the position vector, and J_{T} completes the right-handed system. The desired pose of the chaser satellite is given by the reference frame D ($I_{\mathrm{D}}, J_{\mathrm{D}}, K_{\mathrm{D}}$), such that in one orbital revolution the desired reference moves in an elliptical manner in the $J_{\mathrm{T}} - K_{\mathrm{T}}$ plane, with a semi-major axis (along K_{T}) length of 20 m, and a semi-minor axis (along J_{T}) length of 10 m. We initialized the desired reference as $\bar{r}^{\mathrm{T}}_{\mathrm{D/T}}(0) = [0, -10, 0]^{\mathsf{T}}$ m and $q_{\mathrm{D/T}}(0) = (0, [1, 0, 0]^{\mathsf{T}})$.

The initial state of the system is given by $q_{\mathrm{B/D}}(0) = (0.7071, [0.7071, 0, 0]^{\mathsf{T}})$, $\bar{r}^{\mathrm{B}}_{\mathrm{B/D}}(0) = [3, 4, 5]^{\mathsf{T}}$ m, $\bar{\omega}^{\mathrm{B}}_{\mathrm{B/D}}(0) = [0.5, 1, 1]^{\mathsf{T}}$ rad/s, $\bar{v}^{\mathrm{B}}_{\mathrm{B/D}}(0) = [0.5, -0.5, 1]^{\mathsf{T}}$ m/s, $\mathrm{v}(M^{\mathrm{B}}) = [5, 2, 3, 5, 1, 4, 10]^{\mathsf{T}}$, $\mathrm{v}(\widehat{M^{\mathrm{B}}})(0) = 0$. The matrix gains were set to $\bar{K}_r = 0.74/3\,\mathbb{I}_3$, $\bar{K}_q = 0.2/3\,\mathbb{I}_3$, $\bar{K}_v = 4.22\,\mathbb{I}_3$, $\bar{K}_\omega = 0.75\,\mathbb{I}_3$, and $K_i = 10\,\mathbb{I}_7$. The final time of the simulation was set to $T = 100$ s, but the full time range is only shown when necessary. The concurrent learning term of the update of the mass matrix is enabled at 0.02s with $\alpha = 0.1$. The relative and absolute tolerances for the solver were set to 10^{-10}. In this simulation, we expect $\boldsymbol{\omega}^{\mathrm{B}}_{\mathrm{B/D}} \to \mathtt{0}$ and $\boldsymbol{q}_{\mathrm{B/D}} \to \mathtt{1}$, while the parameters of the dual mass matrix estimates converge to their true values.

Figure 1 shows the pose of the spacecraft converging to the reference trajectory. Figure 2 shows the angular and linear velocities of the body frame relative to the desired reference frame converging, which combined with the pose converging, ensures that tracking is fulfilled. Figure 3 shows the evolution of the estimate of the dual inertia matrix. For the proposed controller, the parameters converge to their true values in under 20 seconds. In fact, $\mathsf{P}(t) > 0$ from the ninth timestep for which the CL algorithm was enabled, corresponding to $t = 0.0204$ s, but its minimum singular value only becomes $\sigma_{\min}(\mathsf{P}(t)) = 0.1$ at $t = 0.75$ s. The singular values are shown as a function of time in Figure 4. Given the positive definiteness of $\mathsf{P}(t)$, the convergence of the inertia parameters is guaranteed early in the simulation for the proposed controller, while not all parameters converge for the baseline controller, since the persistency of excitation condition is not met for this maneuver. Finally, Figure 5 shows the control effort (i.e., forces and torques) applied at the base of the spacecraft to achieve the control objective, exhibiting no meaningful differences.

An even more challenging problem is that of performing identification during deep-space operations, where the gravitational effects can be neglected. For this example, terms associated to gravity and J_2 are neglected in equations (77) and (81). In this case, the function $\mathrm{W}(t)$ simplifies to $\mathrm{W}(t) = \mathrm{W}_{rb}(t)$, with $\mathrm{W}_{rb} : [0, \infty) \to \mathbb{R}^{8\times 7}$ as

$$\mathrm{W}_{rb}(t)\mathrm{v}(\Delta M^{\mathrm{B}}) \triangleq \boldsymbol{\omega}^{\mathrm{D}}_{\mathrm{D/I}} \times (\Delta M^{\mathrm{B}} \star (\boldsymbol{\omega}^{\mathrm{D}}_{\mathrm{D/I}})^{\mathsf{s}}) + \Delta M^{\mathrm{B}} \star (\dot{\boldsymbol{\omega}}^{\mathrm{D}}_{\mathrm{D/I}})^{\mathsf{s}}. \tag{99}$$

Explicitly,

$$\mathrm{W}_{rb}(t) = \begin{bmatrix} 0_{4\times 6} & \dot{v}^{\mathrm{D}}_{\mathrm{D/I}} + \omega^{\mathrm{D}}_{\mathrm{D/I}} \times v^{\mathrm{D}}_{\mathrm{D/I}} \\ \mathrm{W}_{rb,I}(t) & 0_{4\times 1} \end{bmatrix},$$

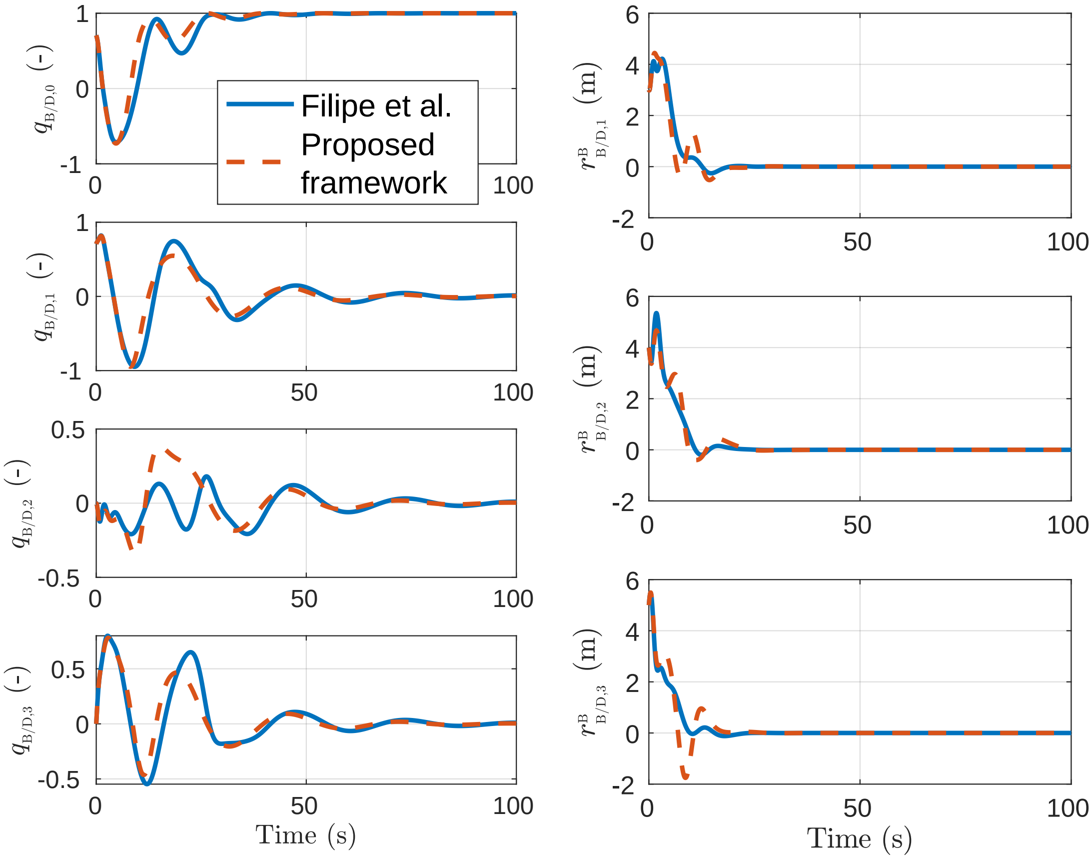

Figure 1. Attitude and position tracking error.

where $\boldsymbol{\omega}^{\mathrm{D}}_{\mathrm{D/I}} = \omega^{\mathrm{D}}_{\mathrm{D/I}} + \epsilon v^{\mathrm{D}}_{\mathrm{D/I}} = (0, [p^{\mathrm{D}}_{\mathrm{D/I}}, q^{\mathrm{D}}_{\mathrm{D/I}}, r^{\mathrm{D}}_{\mathrm{D/I}}]^{\mathsf{T}}) + \epsilon v^{\mathrm{D}}_{\mathrm{D/I}}$ and

$$\mathrm{W}_{rb,I}(t) = \begin{bmatrix} 0 & 0 & 0 & 0 & 0 & 0 \\ \dot{p}^{\mathrm{D}}_{\mathrm{D/I}} & \dot{q}^{\mathrm{D}}_{\mathrm{D/I}} - p^{\mathrm{D}}_{\mathrm{D/I}} r^{\mathrm{D}}_{\mathrm{D/I}} & \dot{r}^{\mathrm{D}}_{\mathrm{D/I}} + p^{\mathrm{D}}_{\mathrm{D/I}} q^{\mathrm{D}}_{\mathrm{D/I}} & -q^{\mathrm{D}}_{\mathrm{D/I}} r^{\mathrm{D}}_{\mathrm{D/I}} & (q^{\mathrm{D}}_{\mathrm{D/I}})^2 - (r^{\mathrm{D}}_{\mathrm{D/I}})^2 & q^{\mathrm{D}}_{\mathrm{D/I}} r^{\mathrm{D}}_{\mathrm{D/I}} \\ p^{\mathrm{D}}_{\mathrm{D/I}} r^{\mathrm{D}}_{\mathrm{D/I}} & \dot{p}^{\mathrm{D}}_{\mathrm{D/I}} + q^{\mathrm{D}}_{\mathrm{D/I}} r^{\mathrm{D}}_{\mathrm{D/I}} & (r^{\mathrm{D}}_{\mathrm{D/I}})^2 - (p^{\mathrm{D}}_{\mathrm{D/I}})^2 & \dot{q}^{\mathrm{D}}_{\mathrm{D/I}} & \dot{r}^{\mathrm{D}}_{\mathrm{D/I}} - p^{\mathrm{D}}_{\mathrm{D/I}} q^{\mathrm{D}}_{\mathrm{D/I}} & -p^{\mathrm{D}}_{\mathrm{D/I}} r^{\mathrm{D}}_{\mathrm{D/I}} \\ -p^{\mathrm{D}}_{\mathrm{D/I}} q^{\mathrm{D}}_{\mathrm{D/I}} & (p^{\mathrm{D}}_{\mathrm{D/I}})^2 - (q^{\mathrm{D}}_{\mathrm{D/I}})^2 & \dot{p}^{\mathrm{D}}_{\mathrm{D/I}} - q^{\mathrm{D}}_{\mathrm{D/I}} r^{\mathrm{D}}_{\mathrm{D/I}} & p^{\mathrm{D}}_{\mathrm{D/I}} q^{\mathrm{D}}_{\mathrm{D/I}} & \dot{q}^{\mathrm{D}}_{\mathrm{D/I}} + p^{\mathrm{D}}_{\mathrm{D/I}} r^{\mathrm{D}}_{\mathrm{D/I}} & \dot{r}^{\mathrm{D}}_{\mathrm{D/I}} \end{bmatrix}.$$

For this example, the time-varying reference was selected as $\bar{\omega}^{\mathrm{D}}_{\mathrm{D/I}}(t) = [0, \sin(t), 0]^{\mathsf{T}}$ and $\bar{v}^{\mathrm{D}}_{\mathrm{D/I}}(t) = [1, 0, 0]^{\mathsf{T}}$. The

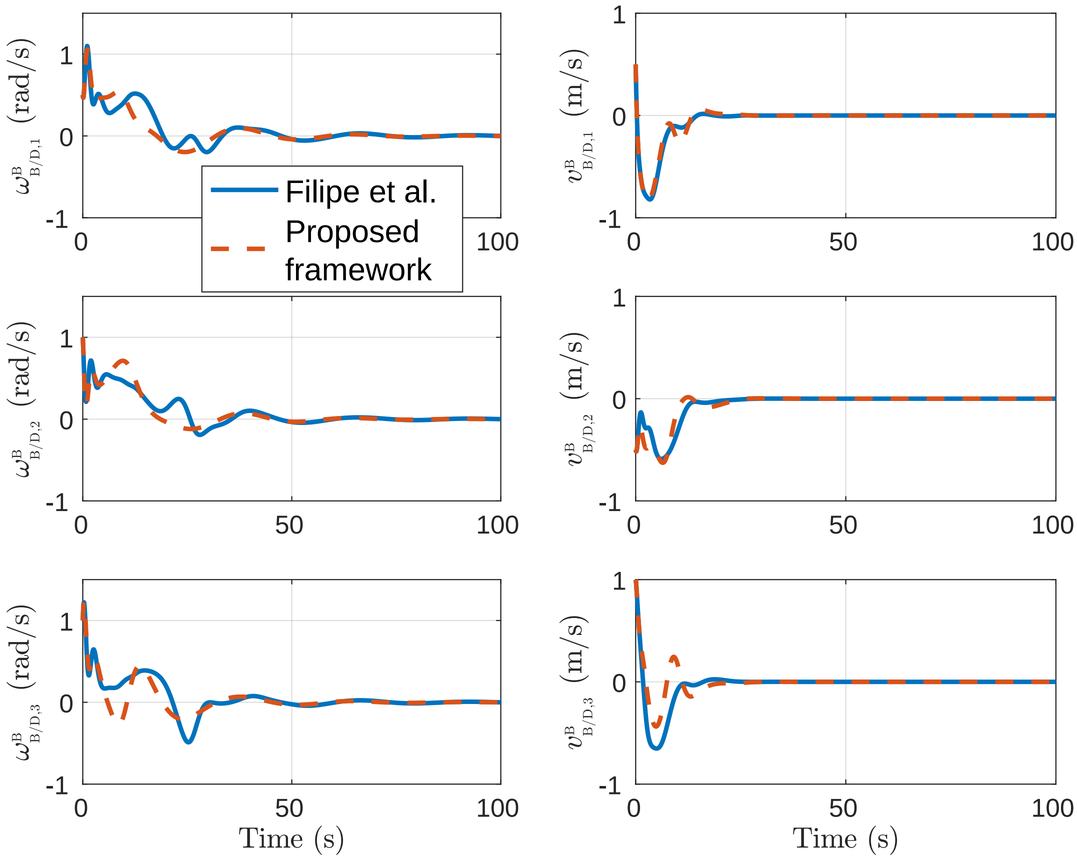

Figure 2. Angular and linear velocity tracking error for formulation.

controller gain is set to $\alpha = 1$. For this particular reference,

$$\mathrm{W}_{rb}(t) = \begin{bmatrix} 0 & 0 & 0 & 0 & 0 & 0 & 1 \\ 0 & 0 & 0 & 0 & 0 & 0 & 0 \\ 0 & 0 & 0 & 0 & 0 & 0 & -\sin(t) \\ 0 & 0 & 0 & 0 & 0 & 0 & 0 \\ 0 & \cos(t) & 0 & 0 & \sin(t)^2 & 0 & 0 \\ 0 & 0 & 0 & \cos(t) & 0 & 0 & 0 \\ 0 & -\sin(t)^2 & 0 & 0 & \cos(t) & 0 & 0 \\ 0 & 0 & 0 & 0 & 0 & 0 & 0 \end{bmatrix}, \tag{100}$$

and

$$\mathrm{W}_{rb}(t)^\intercal \mathrm{W}_{rb}(t) = \mathrm{diag}\left(0, \cos(t)^2 + \sin(t)^4, 0, \cos(t)^2, \cos(t)^2 + \sin(t)^4, 0, \sin(t)^2 + 1\right),$$

which has maximum rank 4. This means that for the baseline controller, the persistency of excitation condition will

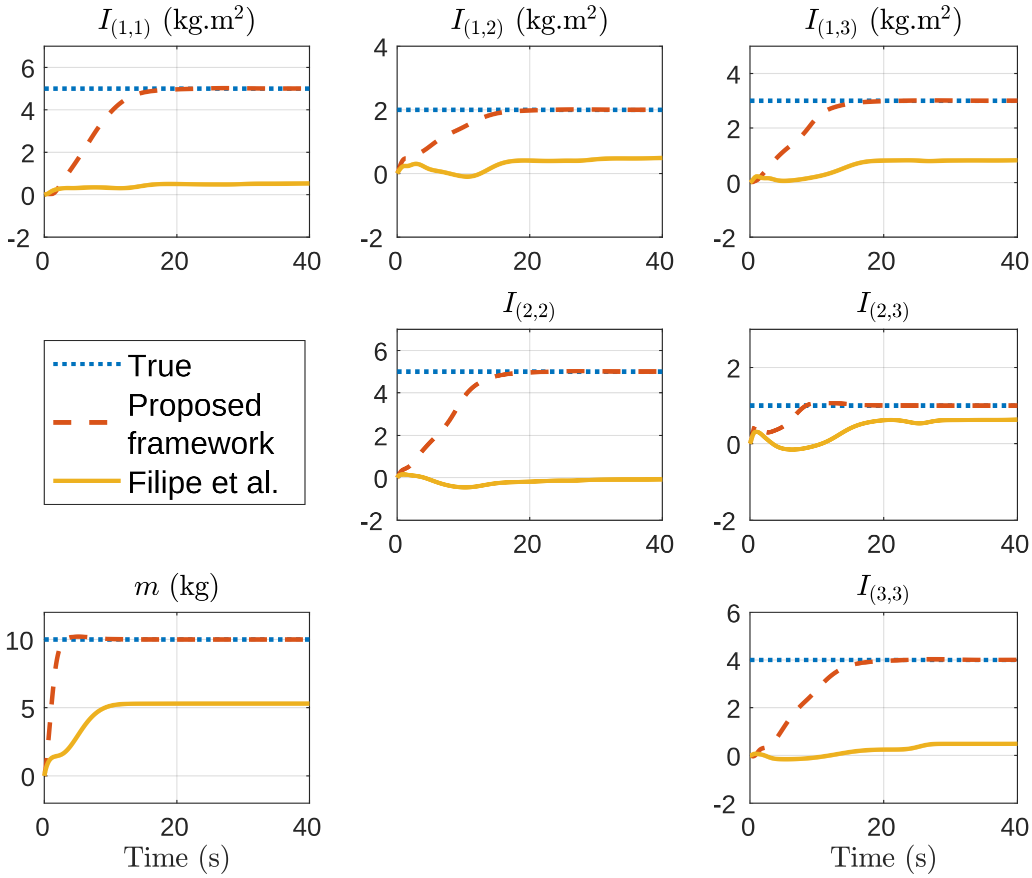

Figure 3. Evolution of estimated dual inertia matrix parameters.

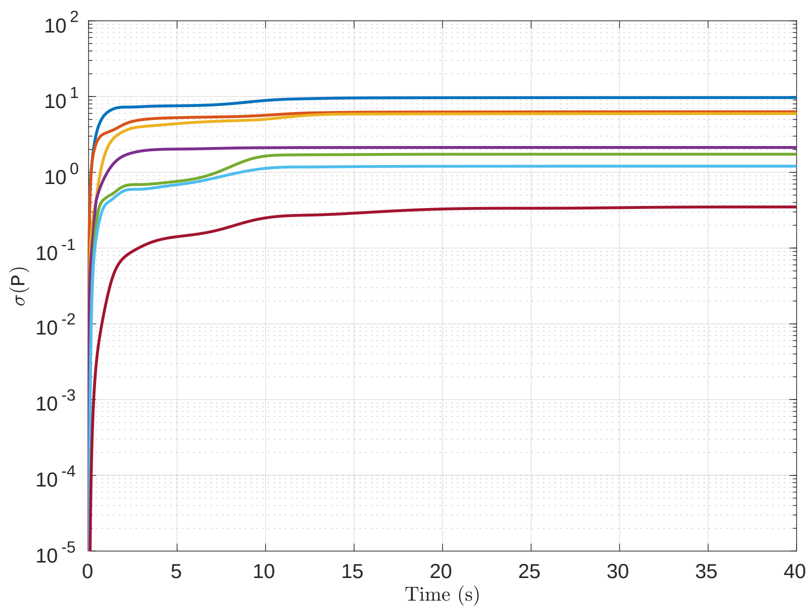

Figure 4. Singular values of matrix $\mathsf{P}(t)$**.**

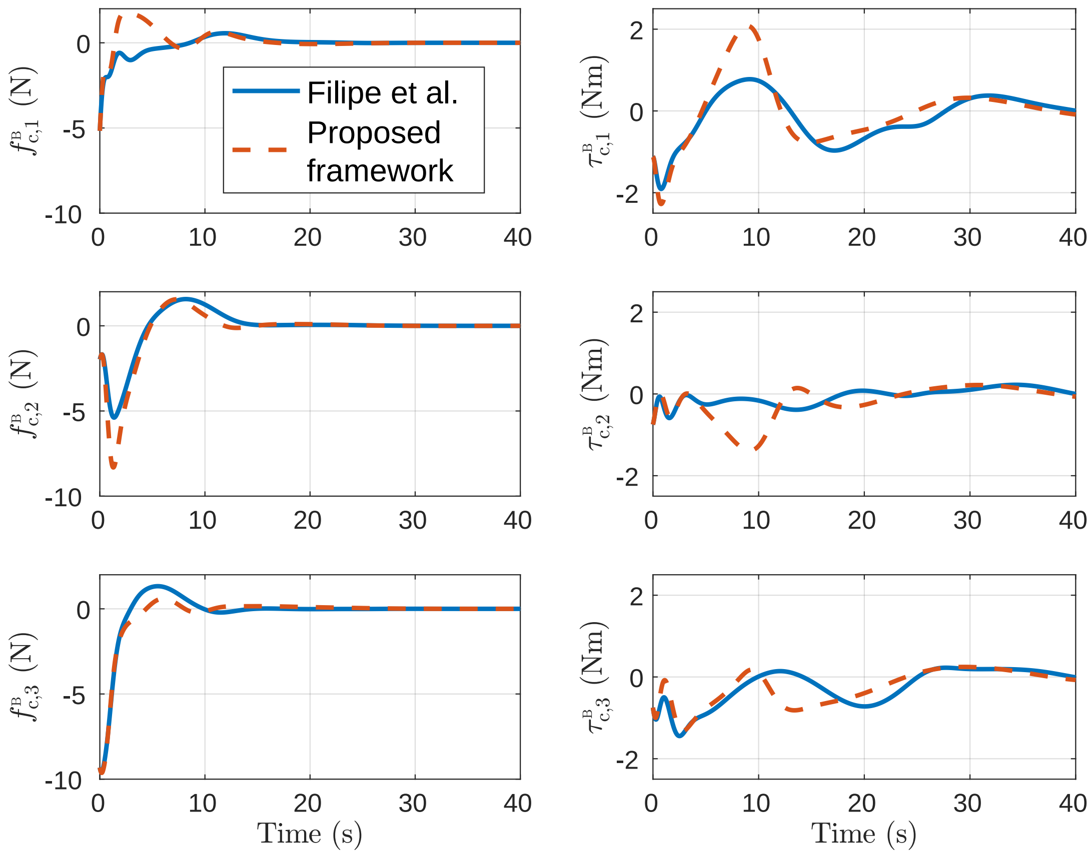

Figure 5. Control effort commanded by the controller.

not be met since we require the condition in equation (98) to be satisfied.

The initial state of the system is given by $q_{\text{B/D}}(0) = (0.872, -[0.118, 0.462, 0.110]^{\intercal})$, $\bar{r}^{\text{B}}_{\text{B/D}}(0) = [1, 2, 0.5]^{\intercal}$ m, $\bar{\omega}^{\text{B}}_{\text{B/D}}(0) = [0.5, 1, 1]^{\intercal}$ rad/s, $\bar{v}^{\text{B}}_{\text{B/D}}(0) = [0.5, -0.5, 1]^{\intercal}$ m/s, $\mathrm{v}(M^{\text{B}}) = [5, 2, 3, 5, 1, 4, 10]^{\intercal}$, $\mathrm{v}(\widehat{M^{\text{B}}})(0) = 0$. The matrix gains were set to $\bar{K}_r = 0.74/3\,\mathbb{I}_3$, $\bar{K}_q = 0.2/3\,\mathbb{I}_3$, $\bar{K}_v = 84.37\,\mathbb{I}_3$, $\bar{K}_\omega = 15\,\mathbb{I}_3$, and $K_i = 10\,\mathbb{I}_7$. The final time of the simulation was set to $T = 50$ s. The concurrent learning term of the update of the mass matrix is enabled at the beginning of the simulation with $\alpha = 1$.

Figure 6 shows the attitude and the pose of the body frame with respect to the desired frame, while figure 7 shows the angular and linear velocities. In both cases, both controllers converge onto the desired reference trajectory. Figure 8 shows the time evolution of the mass parameters. We can observe that only the proposed CL controller converges to the true values, even though the reference itself is not persistently exciting enough. The reasoning for this is that, through integration of other dynamic information, the CL controller has gathered enough information during the initial transient to adapt correctly the estimates. Finally, figure 9 shows the singular values of the matrix $\mathsf{P}(t)$. We can observe that this matrix achieves the full rank condition rather quickly. Forces and torques for the maneuver are shown in figure 10.

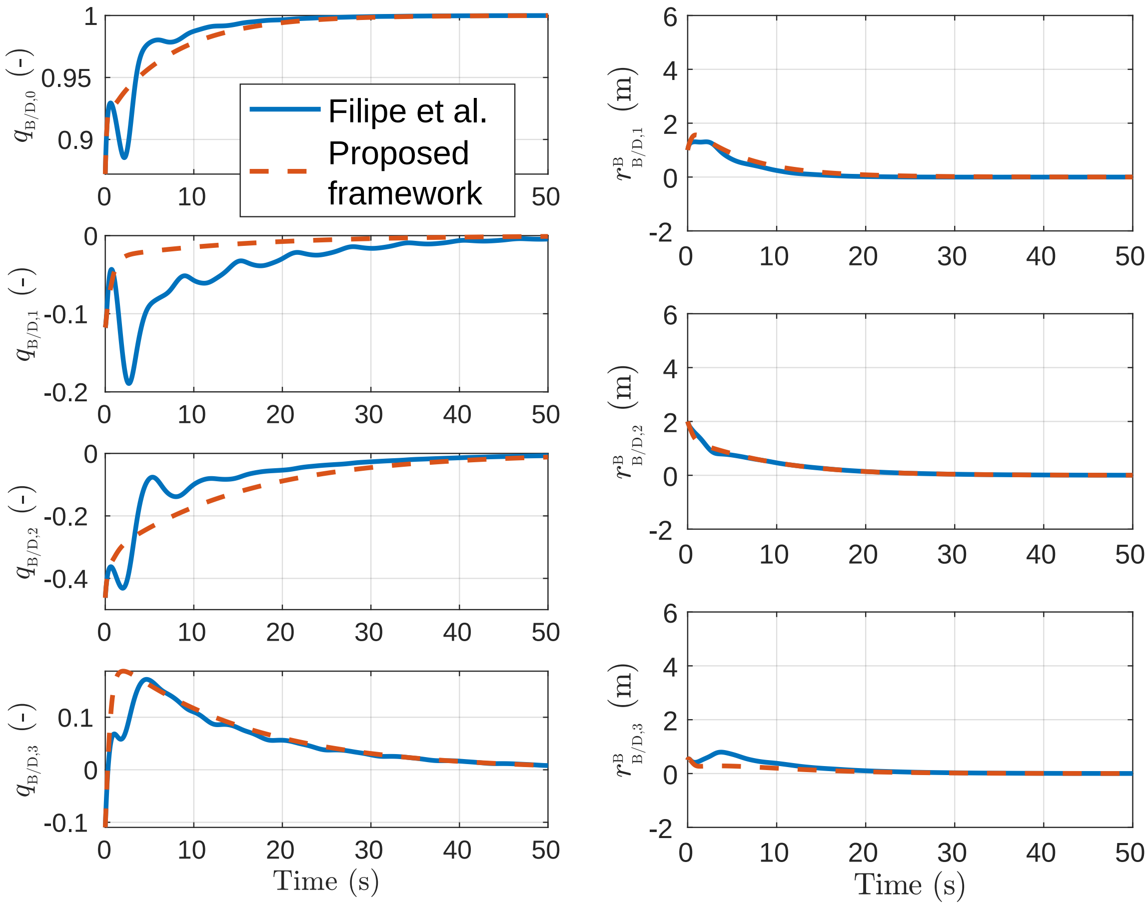

Figure 6. Attitude and position tracking error - deep space maneuver.

It should be mentioned that the concurrent learning algorithm requires knowledge of the forces and torques applied about the center of mass of the body, i.e., knowledge of $\boldsymbol{f}^{\mathrm{B}} = f^{\mathrm{B}} + \epsilon\tau^{\mathrm{B}}$. In our simulations, this quantity was obtained from the output of the controller, so the concurrent learning term is constructed from data from the previous timestep. In practice, these quantities are not trivial to obtain and it will require that the actuators and body disturbances are properly characterized. Preliminary results for research show that taking the output of the controller in the case of mild, additive Gaussian disturbances at the input is a reasonable strategy.

CONCLUSION

In this paper we have provided a brief introduction to Clifford Algebras and their relationship to the well-known quaternion and dual quaternion algebras, which are used extensively in spacecraft control problems. This was followed by an extensive list of control and estimation algorithms that arose in the context of quaternion algebra for attitude control and estimation, but which posses natural counterparts in dual quaternion algebra for pose control and estimation. The formulations exploit the passive nature of mechanical systems and the many parallelisms between the quaternion

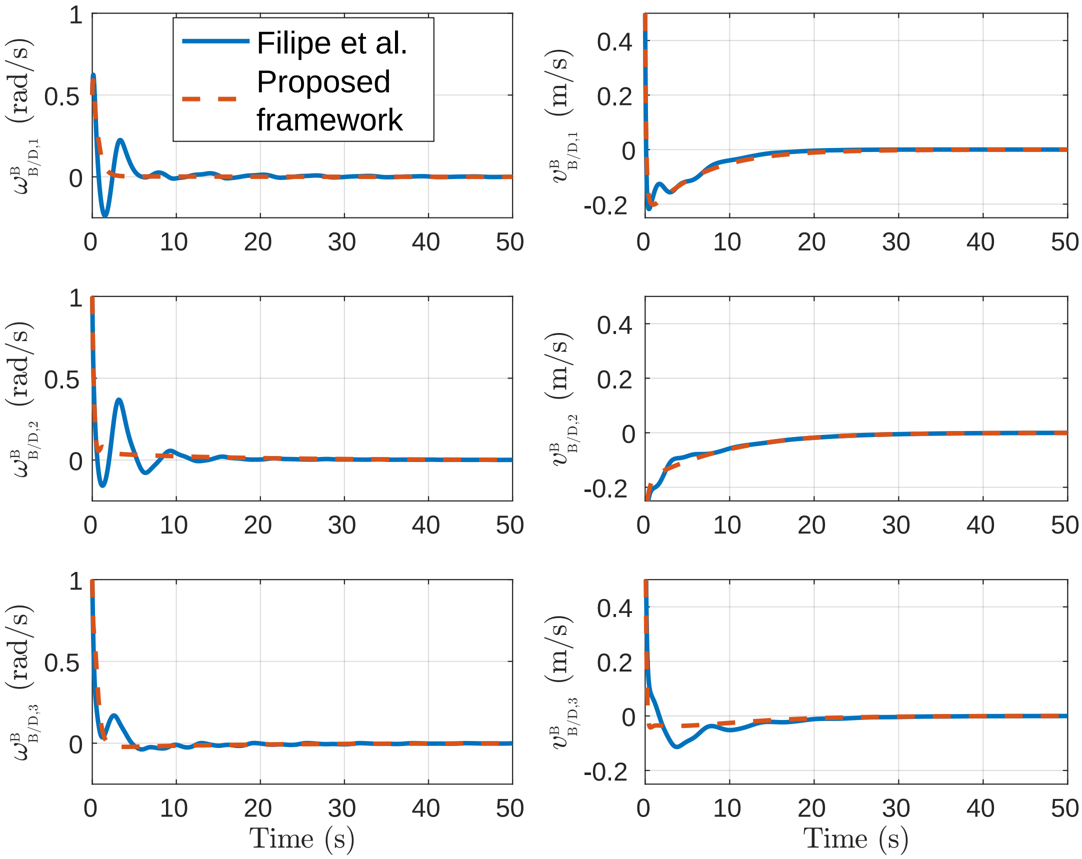

Figure 7. Angular and linear velocity tracking error for formulation - deep space maneuver.

and the dual quaternion algebras – including the representation of kinematics and dynamics for 3-DOF and 6-DOF motion, respectively.

Additionally, we presented a new adaptive pose-tracking controller in terms of dual quaternions. Continuous-time concurrent learning was incorporated to yield stronger assurances on the convergence of the mass and inertia properties of the spacecraft than a controller that relies solely on a persistently exciting reference motion. The relationship between the rank condition that arises in concurrent learning and the integral relationship that ensures parameter convergence in the context of persistency of excitation was studied in greater detail. It was shown that the concurrent learning rank condition is a contributing factor to ensure persistency of excitation, but that the rank condition (concurrent learning) and the integral condition (persistency of excitation) are not dissociated. As far as the authors are aware, this is the first time a continuous formulation of concurrent learning is proposed, which allowed for the relationship between persistency of excitation and the CL rank condition to be elucidated. Finally, the proposed adaptive controller was evaluated against a baseline controller that does not include the concurrent learning term, confirming the parameter estimation results in simulation.

Current and future work in dual quaternions will aim at modeling spacecraft-mounted robotic manipulators using

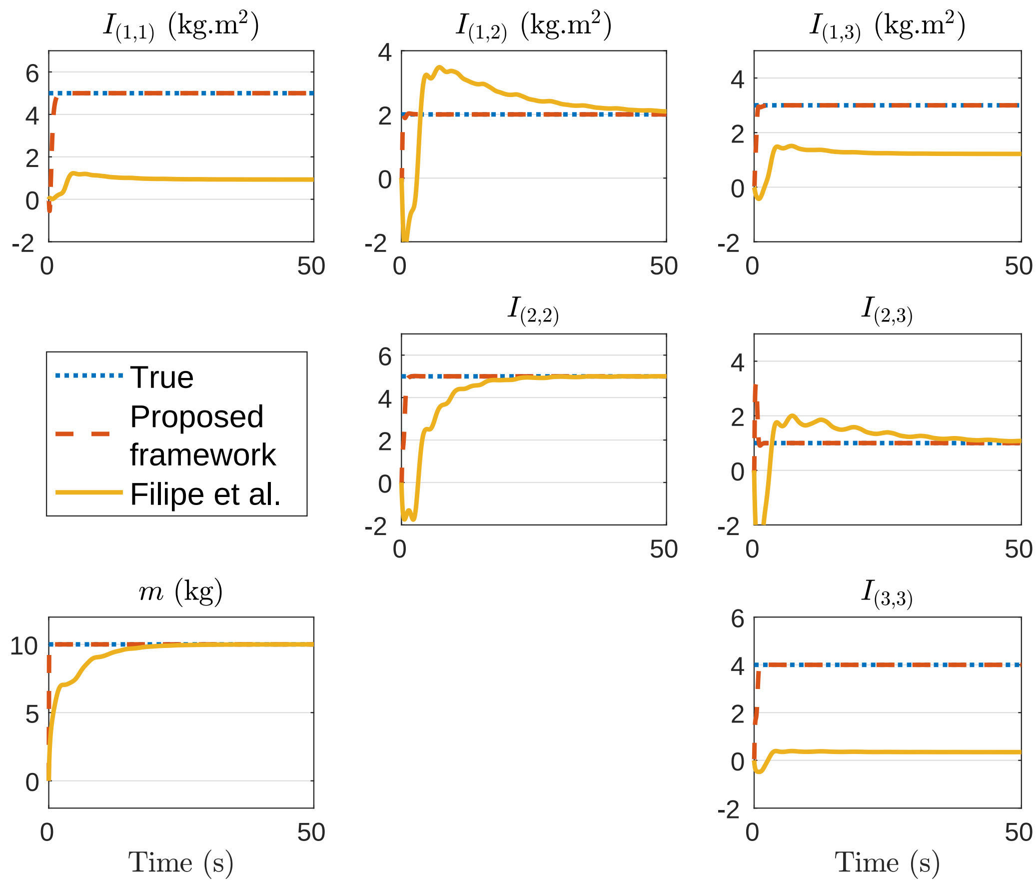

Figure 8. Evolution of estimated dual inertia matrix parameters - deep space maneuver.

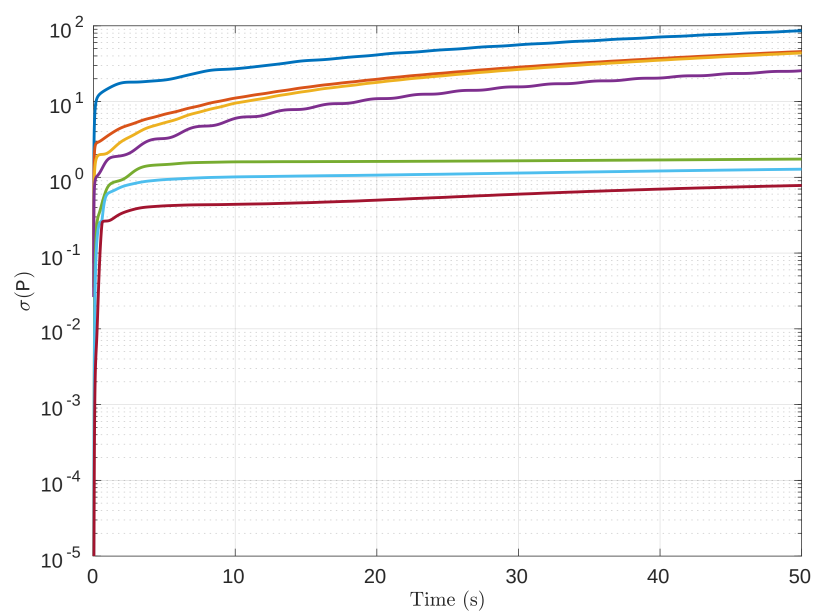

Figure 9. Singular values of matrix P(t) **- deep space maneuver.**

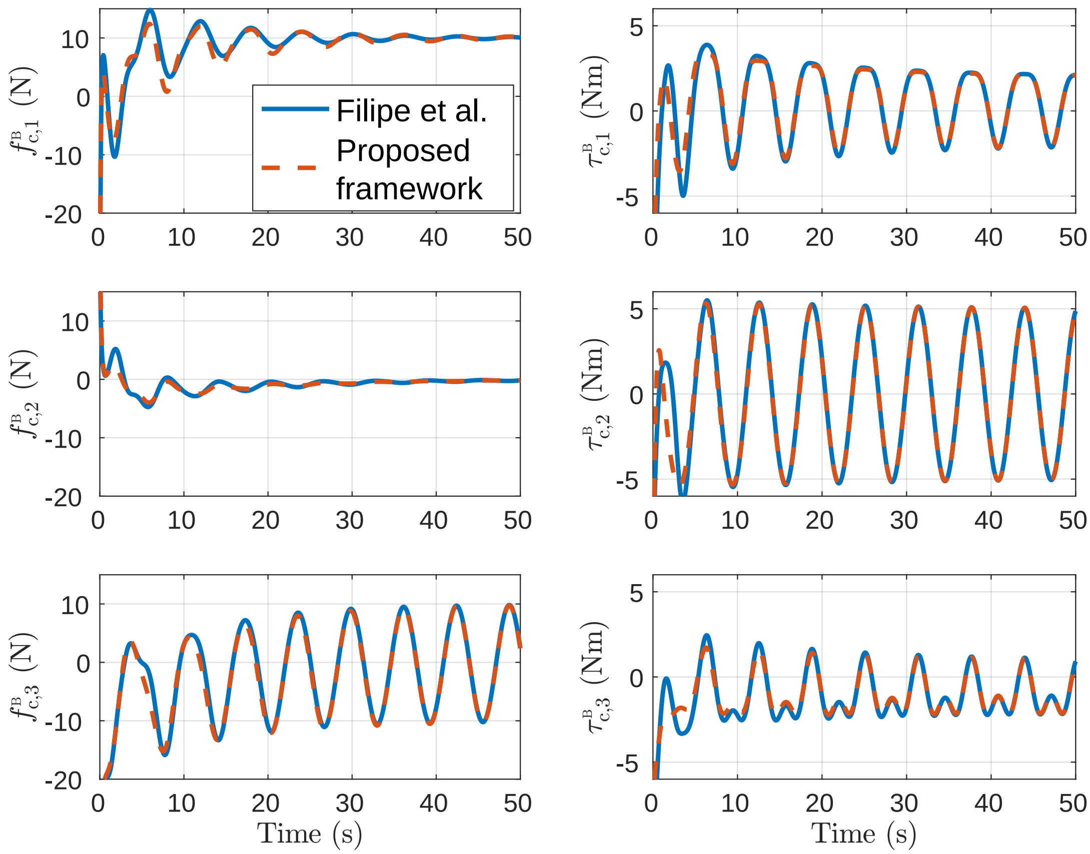

Figure 10. Control effort commanded by the controller - deep space maneuver.

a Newton-Euler approach, with the purpose of providing a unified algebraic framework to perform a wide range of spacecraft GNC functions during in-orbit robotic servicing.

CONFLICT OF INTEREST

The authors confirm that there are no conflicts of interest related to the contents of this work.

REFERENCES

[1] M. Oda, "Space Robot Experiments on NASDA's ETS-VII Satellite - Preliminary Overview of the Experiment Results," *Proceedings 1999 IEEE International Conference on Robotics and Automation*, Vol. 2, Detroit, Michigan, United States, May 1999, pp. 1390–1395 vol.2, 10.1109/ROBOT.1999.772555.

[2] M. Oda, "ETS-VII: Achievements, Troubles and Future," *Proceedings of the 6th International Symposium on Artificial Intelligence and Robotics & Automation in Space (i-SAIRAS)*, St.-Hubert, Quebec, Canada, Canadian Space Agency, June 2001.

[3] A. Ogilvie, J. Allport, M. Hannah, and J. Lymer, "Autonomous Satellite Servicing Using the Orbital Express Demonstration Manipulator System," *Proceedings of the Ninth International Symposium on Artificial Intelligence Robotics and Automation in Space, iSAIRAS*, Los Angeles, U.S.A., Feb 26–29 2008.

[4] K. Yoshida, "Achievements in Space Robotics," *IEEE Robotics & Automation Magazine*, Vol. 16, Dec 11 2009, pp. 20–28, 10.1109/mra.2009.934818.

[5] C. G. Henshaw, "NRL Robotics Overview," Online, July 2009. Future In-Space Operations (FISO) Colloquium.

[6] G. Roesler, "Robotic Servicing of Geosynchronous Satellites (RSGS) Program Overview," Online, June 2016. Future In-Space Operations (FISO) Colloquium.

[7] B. B. Reed, "NASA Satellite Servicing Evolution," Online, Jan. 2017. Future In-Space Operations (FISO) Colloquium.

[8] B. B. Reed, R. C. Smith, B. J. Naasz, J. F. Pellegrino, and C. E. Bacon, "The Restore-L Servicing Mission," *AIAA SPACE Forum*, Long Beach, California, Sep 13 – 16 2016, 10.2514/6.2016-5478.

[9] D. Dimitrov, *Dynamics and Control of Space Manipulators During a Satellite Capturing Operation*. PhD thesis, Tohoku University, Feb. 2005.

[10] S. Xu, H. Wang, D. Zhang, and B. Yang, "Extended Jacobian Based Adaptive Zero Reaction Motion Control for Free-floating Space Manipulators," *Proceedings of the 33rd Chinese Control Conference*, Nanjing, China, July 28-30 2014, 10.1109/chicc.2014.6896402.

[11] V. Dubanchet, D. Saussié, D. Alazard, C. Bérard, and C. L. Peuvédic, "Modeling and Control of a Space Robot for Active Debris Removal," *CEAS Space Journal*, Vol. 7, No. 2, 2015, pp. 203–218, 10.1007/s12567-015-0082-4.

[12] J. Dooley and J. McCarthy, "Spatial Rigid Body Dynamics using Dual Quaternion Components," *Proceedings 1991 IEEE International Conference on Robotics and Automation*, Sacramento, California, April 9-11 1991, pp. 90–95.

[13] V. Brodsky and M. Shoham, "Dual numbers representation of rigid body dynamics," *Mechanism and Machine Theory*, Vol. 34, July 1999, pp. 693–718. Erratum for this paper has been published.

[14] J. Wang and Z. Sun, "6–DOF robust adaptive terminal sliding mode control for spacecraft formation flying," *Acta Astronautica*, Vol. 73, 2012, pp. 76 – 87, 10.1016/j.actaastro.2011.12.005.

[15] J.-Y. Wang, H.-Z. Liang, Z.-W. Sun, S.-N. Wu, and S.-J. Zhang, "Relative Motion Coupled Control Based on Dual Quaternion," *Aerospace Science and Technology*, Vol. 25, March 2013, pp. 102 – 113, 10.1016/j.ast.2011.12.013.

[16] X. Wang and C. Yu, "Unit-Dual-Quaternion-Based PID Control Scheme for Rigid-Body Transformation," *Proceedings of the 18th IFAC World Congress*, Milan, Italy, August 28 - September 2 2011.

[17] J. Wang, H. Liang, Z. Sun, S. Zhang, and M. Liu, "Finite-Time Control for Spacecraft Formation with Dual-Number-Based Description," *Journal of Guidance, Control, and Dynamics*, Vol. 35, May 2012, pp. 950–962, 10.2514/1.54277.

[18] N. Filipe and P. Tsiotras, "Rigid Body Motion Tracking Without Linear and Angular Velocity Feedback Using Dual Quaternions," *European Control Conference*, Zürich, Switzerland, July 17–19 2013, pp. 329–334.

[19] N. Filipe and P. Tsiotras, "Adaptive Model-Independent Tracking of Rigid Body Position and Attitude Motion with Mass and Inertia Matrix Identification using Dual Quaternions," *AIAA Guidance, Navigation, and Control Conference*, AIAA 2013-5173, Boston, MA, August 19–22 2013, 10.2514/6.2013-5173.

[20] N. Filipe and P. Tsiotras, "Adaptive Position and Attitude-Tracking Controller for Satellite Proximity Operations Using Dual Quaternions," *Journal of Guidance, Control, and Dynamics*, Vol. 38, 2014, pp. 566–577, 10.2514/1.G000054.

[21] N. Filipe, A. Valverde, and P. Tsiotras, "Pose Tracking Without Linear and Angular-Velocity Feedback using Dual Quaternions," *IEEE Transactions on Aerospace and Electronic Systems*, Vol. 52, No. 1, 2016, pp. 411–422.

[22] D. Seo, "Fast Adaptive Pose Tracking Control for Satellites via Dual Quaternion Upon Non-Certainty Equivalence Principle," *Acta Astronautica*, Vol. 115, 2015, pp. 32–39, 10.1016/j.actaastro.2015.05.013.

[23] U. Lee and M. Mesbahi, "Dual Quaternions, Rigid Body Mechanics, and Powered-Descent Guidance," *51st IEEE Conference on Decision and Control*, Maui, Hawaii, December 10–13 2012, pp. 3386–3391.

[24] U. Lee and M. Mesbahi, "Dual Quaternion Based Spacecraft Rendezvous with Rotational and Translational Field of View Constraints," *AIAA/AAS Astrodynamics Specialist Conference*, San Diego, CA, August 4 – 7 2014, 10.2514/6.2014-4362.

[25] U. Lee and M. Mesbahi, "Optimal Power Descent Guidance with 6-DoF Line of Sight Constraints via Unit Dual Quaternions," *AIAA Guidance, Navigation, and Control Conference*, January 5–9 2015, 10.2514/6.2015-0319.

[26] W. Hamilton, *Elements of Quaternions*. London: Longmans, Green, & Company, 1866.

[27] N. Filipe and P. Tsiotras, "Simultaneous Position and Attitude Control Without Linear and Angular Velocity Feedback Using Dual Quaternions," *Proceedings of the 2013 American Control Conference*, Washington, DC, June 17–19 2013, pp. 4815–4820.

[28] N. Filipe, *Nonlinear Pose Control and Estimation for Space Proximity Operations: An Approach Based on Dual Quaternions*. PhD thesis, Georgia Institute of Technology, 2014.

[29] D. Hestenes and R. Ziegler, "Projective geometry with Clifford algebra," *Acta Applicandae Mathematica*, Vol. 23, Apr 1991, pp. 25–63, 10.1007/BF00046919.

[30] L. A. Radavelli, E. R. De Pieri, D. Martins, and R. Simoni, "Points, Lines, Screws and Planes in Dual Quaternions Kinematics," *Advances in Robot Kinematics* (J. Lenarcic and O. Khatib, eds.), pp. 285–293, Springer, 2014, 10.1007/978-3-319-06698-1_30.

[31] N. Filipe and P. Tsiotras, "Adaptive Position and Attitude Tracking Controller for Satellite Proximity Operations using Dual Quaternions," *AAS/AIAA Astrodynamics Specialist Conference*, AAS 13-858, Hilton Head, South Carolina, August 11–15 2013, pp. 2313–2332.

[32] F. Lizarralde and J. T. Wen, "Attitude Control Without Angular Velocity Measurement: A Passivity Approach," *IEEE Transactions on Automatic Control*, Vol. 41, March 1996, pp. 468–472.

[33] J. T.-Y. Wen and K. Kreutz-Delgado, "The Attitude Control Problem," *IEEE Transactions on Automatic Control*, Vol. 36, October 1991, pp. 1148–1162.

[34] J. Ahmed, V. T. Coppola, and D. S. Bernstein, "Adaptive Asymptotic Tracking of Spacecraft Attitude Motion with Inertia Matrix Identification," *Journal of Guidance, Control, and Dynamics*, Vol. 21, September-October 1998, pp. 684–691, 10.2514/2.4310.

[35] E. Lefferts, F. Markley, and M. Shuster, "Kalman Filtering for Spacecraft Attitude Estimation," *Journal of Guidance, Control, and Dynamics*, Vol. 5, September-October 1982, pp. 417–429.

[36] N. Filipe, M. Kontitsis, and P. Tsiotras, "Extended Kalman Filter for Spacecraft Pose Estimation Using Dual Quaternions," *Journal of Guidance, Control, and Dynamics*, Vol. 38, September 2015, pp. 1625 – 1641.

[37] N. Filipe, M. Kontitsis, and P. Tsiotras, *From Attitude Estimation to Pose Estimation Using Dual Quaternions*, ch. 8, pp. 129–143. Taylor & Francis, 2016.

[38] A. Valverde, N. Filipe, M. Kontitsis, and P. Tsiotras, "Experimental Validation of an Inertia-Free Controller and a Multiplicative EKF for Pose Tracking and Estimation Based on Dual Quaternions," *38th AAS Guidance and Control Conference*, No. 2015–017, Breckenridge, CO, January 30 - February 4 2015.

[39] B. P. Malladi, E. A. Butcher, and R. G. Sanfelice, "Robust Hybrid Global Asymptotic Stabilization of Rigid Body Dynamics using Dual Quaternions," *AIAA Guidance, Navigation, and Control Conference, AIAA SciTech Forum*, Jan 8 – 12 2018, 10.2514/6.2018-0606.

[40] J. Yuan, X. Hou, C. Sun, and Y. Cheng, "Fault-tolerant Pose and Inertial Parameters Estimation of an Uncooperative Spacecraft Based on Dual Vector Quaternions," *Proceedings of the Institution of Mechanical Engineers, Part G: Journal of Aerospace Engineering*, jan 2018, pp. 1–20, 10.1177/0954410017751766.

[41] Y. Deng, Z. Wang, and L. Liu, "Unscented Kalman Filter for Spacecraft Pose Estimation Using Twistors," *Journal of Guidance, Control, and Dynamics*, Vol. 39, June 2014, pp. 1844–1856, 10.2514/1.G000368.

[42] G. V. Chowdhary, *Concurrent Learning for Convergence in Adaptive Control Without Persistency of Excitation*. PhD thesis, Georgia Institute of Technology, 2010.

[43] B.-E. Jun, D. S. Bernstein, and N. H. McClamroch, "Identification of the Inertia Matrix of a Rotating Body Based on Errors-in-variables Models," *International Journal of Adaptive Control and Signal Processing*, Vol. 24, No. 3, 2010, pp. 203–210, 10.1002/acs.1112.

[44] G. V. Chowdhary and E. N. Johnson, "Theory and Flight-Test Validation of a Concurrent-Learning Adaptive Controller," *Journal of Guidance, Control, and Dynamics*, Vol. 34, Mar. 2011, pp. 592–607, 10.2514/1.46866.